ETC HE Report 2025/11

New AIR indicator based on POD_Y – proposal of its part related to crops

Authors:
Jan Horálek (CHMI), Leona Vlasáková (CHMI), Nina Benešová (CHMI), Frédéric Tognet (INERIS), Pavel Kurfürst (CHMI)

European Environment Agency
European Topic Centre
Human health and the environment

Cover design: EEA
Cover image: Wheat field. Downloaded from Pixabay.
Layout: EEA / ETC HE (CHMI)

Publication Date: 15.04.2026

DOI: 10.5281/zenodo.19482500

EEA activity: Human health and the environment

How to cite this report:
Horálek, J., Vlasáková, L., Benešová, N., Tognet, F., & Kurfürst, P. (2026). New AIR Indicator based on PODY – proposal of its part related to crops. ETC HE Report 2025/11 (Version 1). Zenodo. https://doi.org/10.5281/zenodo.19482500
The report is available from https://www.eionet.europa.eu/etcs/all-etc-reports and https://zenodo.org/communities/eea-etc/?page=1&size=20.

ETC HE coordinator: Stiftelsen NILU, Kjeller, Norway (https://www.nilu.com/)

ETC HE consortium partners: Federal Environment Agency/Umweltbundesamt (UBA), Aether Limited, Czech Hydrometeorological Institute (CHMI), Institut National de l'Environnement Industriel et des Risques (INERIS), Swiss Tropical and Public Health Institute (Swiss TPH), Universitat Autònoma de Barcelona (UAB), Vlaamse Instelling voor Technologisch Onderzoek (VITO), 4sfera Innova S.L.U., klarFAKT e.U.

European Topic Centre on
Human health and the environment (ETC HE)
https://www.eionet.europa.eu/etcs/etc-he

Contents

Acknowledgements

The ETC HE task manager was Jan Horálek (CHMI, Czechia). The EEA project manager was Alberto González Ortiz. The main author of Chapter 5 was Frédéric Tognet (INERIS, France). The exposure tables for alternative option of the new indicator were calculated by Markéta Schreiberová (CHMI).

The external task ETC HE reviewer was Joana Soares (NILU, Norway). The external reviewers were Ignacio González Fernández and Isaura Rábago (CIEMAT, Spain). Their different comments and suggestions have been included in the document.

Summary

Ground-level ozone (O_3) is considered the most damaging common air pollutant to vegetation, negatively impacting ecosystems, crop yields and forest health. O_3 enters plant leaves through stomata and reacts rapidly in intercellular spaces.

The European air quality standard for vegetation protection, as defined in the Ambient Air Quality Directive (EU, 2024), is based on O_3 indicator AOT40, which is the accumulated O_3 concentration over 80 µg/m^3 in a given period. Annually, the European Environmental Agency (EEA) prepares and publishes the AQ indicator *AIR004 – Exposure of European´s ecosystem to ozone* (EEA, 2025b). This indicator is based on the AOT40 metrics, and more specifically, on the AOT40 maps prepared by the ETC HE (Horálek et al., 2024). It consists of two parts, i.e. the exposure to ozone of agricultural areas (based on the AOT40 for vegetation) and of forested areas (based on the AOT40 for forests).

Although widely used, AOT40 is not biologically optimal for assessing O_3 risk, as it does not consider stomatal uptake or any environmental factors affecting the O_3 uptake via stomata. It is widely acknowledged that O_3-induced damage is more closely related to stomatal uptake than to ambient concentrations. Consequently, a flux-based metric such as Phytotoxic Ozone Dose (POD_Y), which quantifies the accumulated stomatal O_3 flux above a threshold Y, provides a more accurate measure of O_3 exposure than AOT40.

This report proposes a new indicator based on POD_Y as complementary information to the current EEA indicator *AIR004*. Similarly to the AIR004, the new POD_Y-based indicator should also show the O_3 exposure of crops and forests separately. This report develops the first part of the new indicator, which is related to the flux-related O_3 exposure of crops. The flux-related O_3 exposure of forest trees is planned to be developed in 2026.

Two options of the new indicator related to the crops are considered, i.e. the crop specific POD_Y indicator and a more generic metric based on the POD_Y used in the Integrated Assessment Modelling (i.e. POD_YIAM), which can be applied for different crops. The advantage of the crop specific POD_Y metric is in its more exact estimation of the O_3 impacts on the corresponding crop, however, it should be applied only to areas covered by this specific crop. On the other hand, the POD_YIAM is more suitable for estimating the O_3 impacts on the wide variety of crops, and thus it can be applied to areas covered by crops in general. For this reason, the metric POD_3IAM for crops is recommended to be used in the POD_Y-based indicator for crops.

In this report, the POD_3IAM for crops is applied as a basic option for this new indicator. Its results for 2022 and 2023 are presented and analysed. Additionally, as an alternative option, the crop specific metrics POD_6 for wheat and potato are also applied. Subsequently, the results of these two options are compared mutually and with the current AIR004 indicator based on the AOT40 for vegetation metric. Based on the results and their analysis, it is concluded that the new AIR indicator based on POD_Y should complement the current AIR004 indicator, not substitute it. Apart from that, it is concluded that the new indicator based on the POD_3IAM for crops can be fairly used to represent different crop species.

In addition, the reasons for the POD_Y levels and inter-annual differences have been analysed and discussed for POD_Y for wheat, as a case study. It seems that phenology and temperature and also soil moisture in water-limited regions of Europe play a major role in the POD_Y levels, together with the O_3 concentrations.

1 Introduction

Ground-level ozone (referred to as O_3) is a secondary photochemical pollutant formed in complex chain reactions from precursors such as nitrogen oxides (NO_X), volatile organic compounds (VOCs), carbon monoxide (CO), and methane (CH_4). These precursors originate from both natural and anthropogenic sources (Fowler et al., 2008; Anav et al., 2016; Nolle et al., 2002). Since O_3 formation depends on meteorological conditions, its levels fluctuate considerably from year to year (Cox and Chu, 1993; Jacob et al., 1993). As a photochemical pollutant, its presence in the atmosphere is closely linked to solar radiation and high temperatures, which drive its formation (Jacob and Winner, 2009; Coates et al., 2016).

O_3 is considered to be the most damaging common air pollutant to vegetation, negatively impacting crop yields and forest health (Ashmore, 2005; Cieslik, 2009; Fares et al., 2017; EEA, 2020). O_3-induced damage occurs at multiple biological levels, from individual cells and leaves to whole organisms and ecosystems (Fuhrer, 2002; Ashmore, 2005; Ainsworth, 2016; Emberson et al., 2018; Mills et al., 2018). Additionally, elevated O_3 concentrations threaten terrestrial biodiversity and ecosystem services (Mills et al., 2018; Agathokleous et al., 2020; Reif et al., 2023).

O_3 enters plant leaves through stomata and reacts rapidly in intercellular spaces (Fares et al., 2017). Inside the leaf, O_3 diffuses into the apoplast and decomposes into reactive oxygen species (Pell et al., 1997; Schraudner et al., 1997; Mittler, 2002). If a plant's antioxidative system is insufficient, biochemical and physiological changes occurs (Ashmore, 2003; Heath, 2008; Fares et al., 2013; Emberson et al., 2018).

The European air quality standard for vegetation protection, as defined in the Ambient Air Quality Directive (EU, 2024), is based on the accumulated O_3 concentration over a threshold of 40 ppb (AOT40). More precisely, AOT40 is the sum of the difference between hourly concentrations greater than 80 $\mu g/m^3$ (= 40 parts per billion) and 80 $\mu g/m^3$ over a given period using only the one-hour values measured between 8.00 and 20.00 Central European Time (CET) each day, to reflect stomatal activity (Anav et al., 2016). The vegetation period covers April-September for forests and May-July for crops and other vegetation. Note that in EU (2024), only the AOT40 for vegetation (and therefore the period May-July) is considered.

Although widely used, AOT40 is not biologically optimal for assessing O_3 risk, as it does not consider stomatal uptake or any environmental factors affecting the O_3 uptake via stomata (Anav et al., 2016). The stomatal O_3 flux approach, in contrast, accounts for the actual O_3 dose entering the leaf via stomata and factors in key environmental conditions such as phenology, air temperature, soil moisture, vapour pressure deficit (VPD), and solar radiation (Emberson et al., 2000a). High ambient O_3 levels do not necessarily harm plants if stomata are closed due to unfavourable conditions, i.e. high vapour pressure deficit, high temperature and low soil humidity (Paoletti, 2006; Agyei, 2020; Ronan et al., 2020), while lower O_3 concentrations can still cause significant damage when stomata are open (Matyssek et al., 2007; Karlsson et al., 2017).

Thus, scientific consensus suggests that O_3-induced damage is more closely related to stomatal uptake than to ambient concentration (Reich, 1987; Ashmore et al., 2004; Mills et al., 2011). Consequently, a flux-based metric such as Phytotoxic Ozone Dose (POD_Y), which quantifies the accumulated stomatal O_3 flux above a threshold Y, provides a more accurate measure of O_3 exposure than AOT40 (Musselman and Massman, 1998; Nussbaum et al., 2003; Fares et al., 2010; Musselman et al., 2006; Matyssek et al., 2007; Cieslik, 2009). POD_Y has been adopted in the Convention on Long-Range Transboundary Air Pollution (CLRTAP, 2017a; Mills et al., 2011) as a preferred metric. As research advances, further refinement of POD_Y-based metrics will enhance our understanding of O_3 impacts on vegetation and improve mitigation strategies.

Under the European Topic Centres (ETCs, i.e. ETC HE and the previous consortia), the European wide annual air quality (AQ) maps have been routinely constructed since 2005, including the AOT40 maps (Horálek et al., 2024 and references therein). Since 2019, POD_Y maps have also been prepared for different species.

Annually, the European Environmental Agency (EEA) prepares and publishes the AQ indicator *AIR004 – Exposure of European´s ecosystem to ozone* (EEA, 2025b). This indicator is based on the AOT40 metrics, and more specifically, on the AOT40 maps prepared by the ETC HE. It consists of two parts, i.e. the exposure to ozone of agricultural areas (based on the AOT40 for vegetation) and of forested areas (based on the AOT40 for forests).

This report aims to propose a new indicator based on POD_Y as complementary information to the current indicator AIR004. It seems to be appropriate for this POD_Y-based supplementary indicator to consist also of two parts, i.e. one related to the crops and one related to the forests. This report develops the indicator related to the crops, as a first step. The indicator related to the forests (i.e. the second half of the POD_Y-based indicator) will be developed in 2026.

Two options of the new indicator related to the crops are considered, i.e. the crop specific POD_Y indicator and a more generic metric based on the POD_Y used in the Integrated Assessment Modelling (IAM). Next to the proposal of the indicator, the first results of this indicator for years 2022 and 2023 are presented and analysed.

POD_Y is a complex indicator, which depends on different variables. As previously stated, high ambient O_3 concentrations do not necessarily lead to high POD_Y values (for instance, if stomata are closed during unfavourable environmental conditions). Conversely, quite low O_3 concentrations can still lead to fairly high O_3 fluxes when stomata are open under favourable environmental conditions. For that reason, the POD_Y levels and inter-annual differences are in general difficult to be understood. However, if the indicator based on the POD_Y metrics is introduced, the explanation of its levels and inter-annual changes would be important. Thus, this report tries to analyse and discuss the levels and inter-annual differences of POD_6 for wheat (as a case study), in addition to the introduction of the new POD_Y-based indicator.

Chapter 2 discusses two different options for the new POD_Y indicator. Chapter 3 presents the results of the new indicator for 2022 and 2023 for the two discussed options. Chapter 4 compares the results of the two options of the new indicator with the current AIR004 indicator. Chapter 5 analyses the reasons for the POD_Y levels and inter-annual differences. Chapter 6 gives conclusions. Annex 1 explains the methodology, while Annex 2 presents the data used. Annex 3 provides additional results of the POD_Y analysis (as introduced in Chapter 5) at the level of biogeographical regions.

2 Considerations on the new POD_Y-based indicator

The current EEA indicator *AIR004 – Exposure of Europe´s ecosystem to ozone* (EEA, 2025b) consists of two parts, i.e. (i) Exposure of agricultural areas to ozone and (ii) Exposure of forest areas to ozone. The indicator presents two figures (Figures 2.1 and 2.2), which show the exposure of agricultural and forested areas to different values (in terms of limited number of concentration classes) of the ozone indicators AOT40 for vegetation and AOT40 for forests, respectively.

Figure 2.1 Indicator AIR004, Exposure of agricultural areas to ozone in EEA member countries

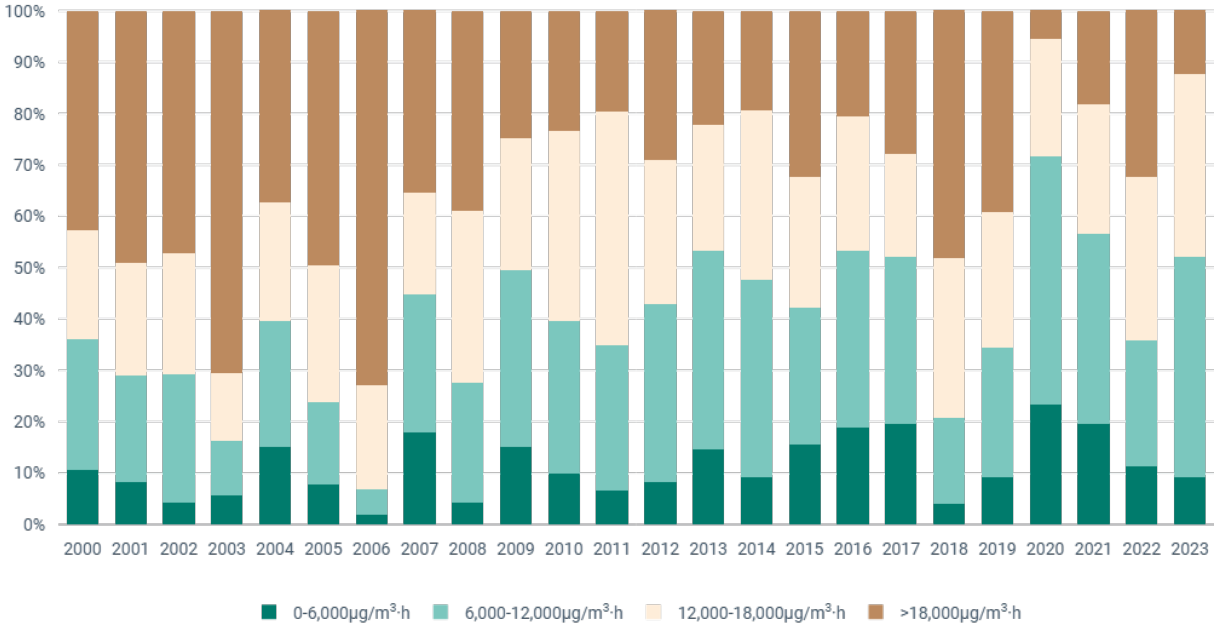

Source: EEA, 2025b

Figure 2.2 Indicator AIR004, Exposure of forest areas to ozone in EEA member countries

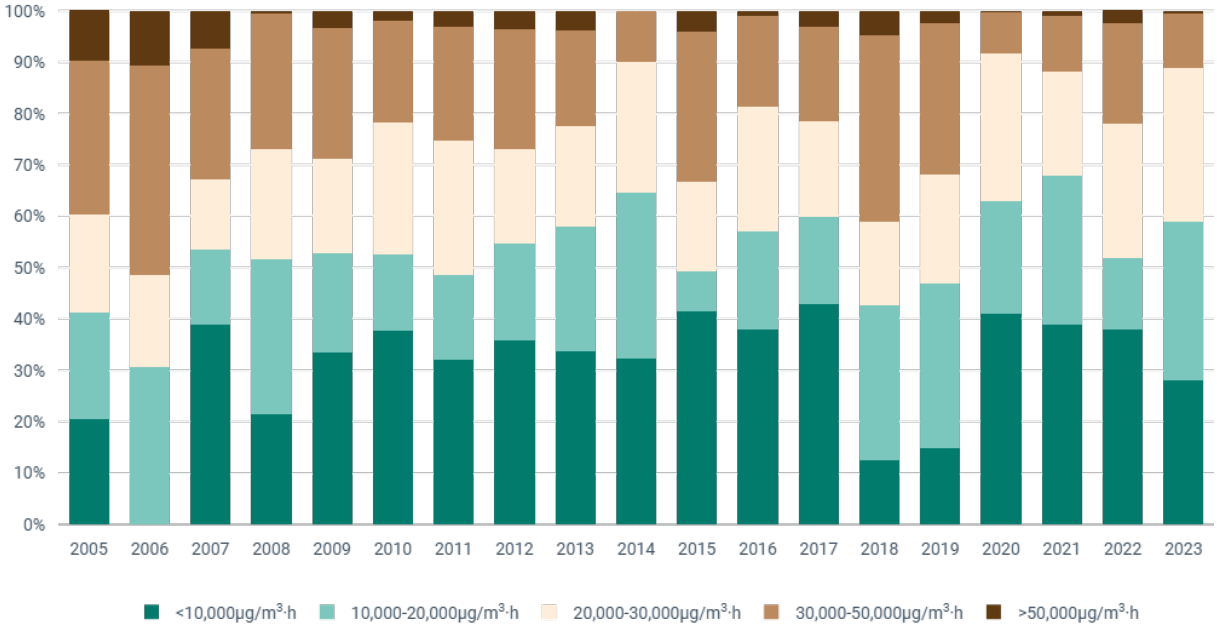

Source: EEA, 2025b

For the agricultural areas exposure estimation, the areas labelled as the CORINE Land Cover (CLC) level-1 class 2 "Agricultural areas" (encompassing the level-2 classes 2.1 "Arable land", 2.2 "Permanent crops", 2.3 "Pastures" and 2.4 "Heterogeneous agricultural areas") are used, while the areas labelled as the CLC level-2 class 3.1 "Forests" are used for the forested areas exposure estimates. The data are presented for a time series starting in 2000 and 2005 for agricultural and forested areas, respectively.

For the exposure of agricultural areas to O_3, four concentration classes of AOT40 for vegetation are used, being the highest one that above the target value (TV) of 18 000 µg/m^3, as set by the EU Ambient Air Quality Directive (EU, 2024); and the lowest one that below the long-term objective (LTO) of 6 000 µg/m^3, as set by the same EU directives. For the exposure of forest areas to O_3, five concentration classes of AOT40 for forests are used, with the lowest being that one below the critical level (CL) of 10 000 µg/m^3 as established by CLRTAP (2024).

As mentioned in the introductory chapter, the O_3-induced effects on vegetation are more closely related to O_3 stomatal uptake than to O_3 ambient concentration. Consequently, the flux-based POD_Y metrics are preferred in risk assessment over the concentration-based AOT40 ones. Thus, it is suggested to complement the current AIR004 indicator with the new indicator based on POD_Y.

Similarly to the current AIR004 indicator, the new POD_Y-based indicator should also show the O_3 exposure of crops and forests separately. This report concentrates on the flux-related O_3 exposure of the crops. The flux-related O_3 exposure of forest trees is planned to be assessed in 2026.

The cumulative stomatal O_3 flux through the stomata of leaves found at the top of the canopy is calculated over the course of the growing season based on ambient O_3 concentration and stomatal conductance to O_3. POD_Y is the accumulated plant uptake (flux) of O_3 above a threshold of Y during a specified time or growth period. Several POD_Y metrics exist (2024), see Box 1. As research advances, further refinement of POD_Y-based metrics will enhance our understanding of O_3 impacts on vegetation and improve mitigation strategies.

Box 1 Metrics for stomatal flux-based critical levels for POD_Y calculation

POD_YSPEC is a species-specific metric that requires extensive input data and is suitable for detailed risk assessment. It represents the phytotoxic O_3 dose above a flux threshold of Y nmol/m² PLA per second for a specific plant species or group of species, accumulated over a defined period during daylight hours. Here, PLA stands for Projected Leaf Area, i.e. the total area of the sides of the leaves that are projected towards the sun.

For crops such as wheat and potato, the Y value is set at 6 nmol/m² PLA per second, as recommended by CLRTAP (2024). The species-specific flux models and associated response functions and critical levels for O_3 sensitive crops and cultivars can be used to quantify the potential negative impacts of O_3 on the security of food supplies at the local and regional scale. They can be used to estimate yield losses, including economic losses. A flux threshold of 6 nmol/m² PLA per second (POD_6SPEC) provides the strongest flux-effect relationships for crops (Pleijel et al., 2007). O_3 effects have been shown to be significant at a 5% reduction of the effect parameter (Mills et al., 2011; Grunhage et al., 2012), forming the basis for determining critical levels (CL) for yield, weight, or quality of grain, tubers, and fruit.

POD_YIAM represents the phytotoxic O_3 dose exceeding a flux threshold of Y nmol/m² PLA per second for a specific vegetation type (like crops and forest trees), designed for large-scale modelling applications such as integrated assessment. It is a vegetation-type-specific metric with lower data requirements, making it well-suited for large-scale modelling and integrated risk assessment. POD_YIAM simplifies stomatal O_3 flux modelling by incorporating species-independent parameters. Despite these simplifications, it remains a robust tool for assessing O_3 risks at regional and global scales.

Source: CLRTAP, 2024

As presented in Box 1, the choice between POD_YSPEC and POD_YIAM depends on data availability and assessment scale, with POD_YSPEC offering high-resolution insights and POD_YIAM enabling broader applicability.

For the new POD_Y-based indicator related to the crops, either a crop specific POD_YSPEC metric can be used or a more generic metric POD_YIAM. If the crop specific POD_YSPEC is considered, POD_6SPEC for wheat might be used, considering wheat as the most representative crop in Europe, potentially supplemented with the POD_6SPEC for potato, considering potato as a representative of the horticultural crops (without regard to its limitations regarding its applicability for the Mediterranean region, for which tomato would be more representative – however, joint use of two different crops for different areas in one European-wide indicator would be quite demanding). If a more generic POD_YIAM is considered, the POD_3IAM for crops can be applied.

The advantage of the crop specific POD_6SPEC metrics is in its more exact estimation of the O_3 impacts on the corresponding crop (wheat or potato). On the other side, the POD_3IAM is probably more suitable for estimating the potential risk of O_3 impacts on the wide variety of crops. Specifically, the POD_6SPEC for wheat and potato (labelled further simply as POD_6 for wheat and potato) should be applied only to areas covered by wheat and potato, respectively. While the POD_3IAM for crops can be applied to areas covered by crops in general.

Further, the POD_3IAM for crops application for the same agricultural areas as for which is applied the current AIR004 indicator (see above) is considered. However, its applicability for pastures (i.e. areas of CLC level-2 class 2.3) should be examined in the future, i.e. whether the use of risk indicators specific for pastures does not lead into a considerable change in areas under the risk of O_3 negative effects.

Based on the above-mentioned facts, the POD_3IAM is further examined for crops as a basic option to be used in the POD_Y-based indicator for crops. The reason is that it can be applied for the same agricultural area as the current AIR004 indicator (with a potential exception for pastures, see above). As an alternative option, the POD_6 for wheat and potato are examined.

3 POD_Y-based indicator related to crops – 2022 and 2023 results

In this chapter, the results of the new POD_Y-based indicator are presented (i.e. its part related to crops) for years 2022 and 2023. Based on the considerations of Chapter 2, the generic metric POD_3IAM for crops is applied as a basic option for this new indicator. Additionally, as an alternative option, the crop specific metrics POD_6 for wheat and potato are also applied.

All POD_Y metrics applied (i.e. POD_3IAM for crops, POD_6 for wheat and POD_6 for potato) have been calculated using the methodology described in CLRTAP (2024), see Annex 1. Specifically, the hourly averaged stomatal O_3 fluxes (F_{sto}) in excess of a Y threshold have been accumulated over a species or vegetation-specific accumulation period, in order to get the phytotoxic O_3 dose above the threshold Y (POD_Y). The stomatal O_3 fluxes (F_{sto}) have been calculated based on the O_3 concentration at the top of the canopy and stomatal conductance (g_{sto}) to O_3. The stomatal conductance (g_{sto}) has been calculated using a multiplicative stomatal conductance model (Emberson et al., 2000a) based on Jarvis (1976) as a function of species-specific maximum g_{sto} (expressed on a projected leaf-area basis), phenology, and prevailing environmental conditions (photosynthetic photon flux density, PPFD), air temperature, vapour pressure deficit (VPD), and soil moisture. The O_3 concentration at the top of the canopy have been calculated based on the ambient O_3 concentrations at the height of the O_3 station measurements, the aerodynamic resistance between the heights of the station measurements and the top of the canopy, the resistance to O_3 diffusion in the laminar sub-layer and other resistances. The ambient O_3 concentrations have been calculated based on O_3 measurement data, O_3 chemical transport modelling (CTM) data, surface solar radiation data and altitude. For details on the methodology and the data used, see Annex 1 and Annex 2, respectively, and Horálek et al. (2024, 2025).

O_3 effects proved to be significant at a 5 % reduction of the effect parameter (Mills et al., 2011), hence critical levels (CL) were determined for this 5 % reduction of the effect parameter (i.e. yield, weight or quality of grain), based on the slope of the function. For CLs as set by CLRTAP, see Annex 1, Table A1.2.

For POD_6 for wheat and potato for 2022 and 2023, the routine spatial maps of these indicators as prepared for Horálek et al. (2024, 2025) have been used. The maps of POD_3IAM for crops have been calculated under the ETC HE for the first time. All maps have been constructed in 0.1° resolution and further converted to 2 km resolution. The maps have been created using the monitoring data from the rural background stations only, based on the assumption there are no areas covered by crop species in urban areas.

The basic option of the new POD_Y-based indicator using the POD_3IAM is presented in Section 3.1. The alternative option of the indicator using the POD_6 for wheat and potato is presented in Section 3.2.

3.1 Basic option: Indicator using generic metric POD_3IAM for crops

At first, the maps of the POD_3IAM for crops have been constructed. Maps 3.1 and 3.2 present the spatial distribution of POD_3IAM for crops in 2022 and 2023. The areas with POD_3IAM for crops values below the CL for crops established by CLRTAP (2024) (i.e. 7.9 mmol/m^2 PLA) are marked in green.

One can see that in most areas, especially those above the CL, the POD_3IAM for crops maps show higher values in 2023 than in 2022 (see also Map 4.1, upper right).

In order to estimate the exposure of crops to O_3 in terms of POD_3IAM, the rural maps of POD_3IAM for crops have been combined with the land cover CLC2018 map in 100 m resolution (EU, 2020). The same agricultural areas as in the current AIR004 indicator have been used, i.e. the areas labelled as the CLC level-1 class 2 “Agricultural areas” (encompassing the level-2 classes 2.1 “Arable land”, 2.2 “Permanent crops”, 2.3 “Pastures” and 2.4 “Heterogeneous agricultural areas”).

Map 3.1 Phytotoxic Ozone Dose – POD_3IAM for crops, rural map, 2022. To be applied only for areas covered by crop species

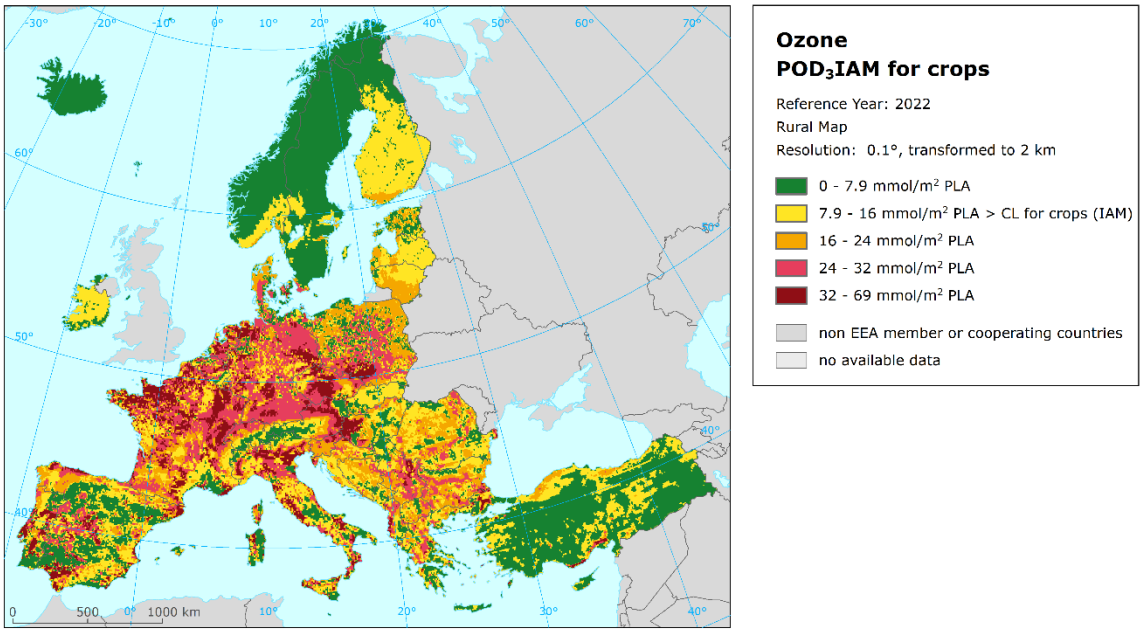

Map 3.2 Phytotoxic Ozone Dose – POD_3IAM for crops, rural map, 2023. To be applied only for areas covered by crop species

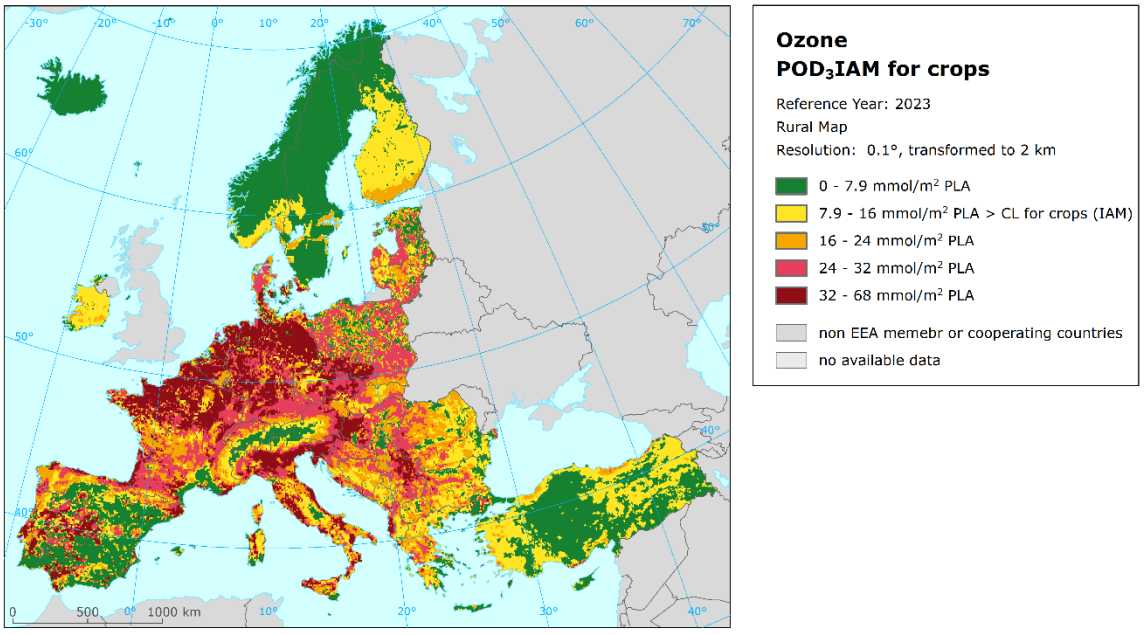

Tables 3.1 and 3.2 present the exposure of crops to O_3 in terms of POD_3IAM for crops for 2022 and 2023, respectively. The tables show the frequency distribution of the agricultural area over some exposure classes for each country, for EU-27, EEA-32, EEA-38 and the total mapping area (with and without Türkiye in the last three cases) and for five large European regions (see Annex 1, Section A1.4). In addition, the absolute and relative agricultural areas where POD_3IAM for crops values are above the CL threshold are presented, as well as the agricultural area weighted concentrations, i.e. the average POD_3IAM values across the agricultural areas.

Table 3.1 Exposure of crops to O_3 and agricultural area weighted concentrations, O_3 indicator POD_3IAM for crops, 2022

Country	Agricultural area, 2022			Fraction of agricultural area, 2022 (%)					Agricultural-weighted POD_3IAM, 2022
	Total area	> CL for crops (7.9 mmol/m² PLA)		< 7.9	7.9-16	16-24	24-32	> 32	
	(km²)	(km²)	(%)	(mmol/m² PLA)					(mmol/m² PLA)
Albania	7,709	6,779	87.9	12.1	22.4	22.8	25.6	17.2	20.8
Andorra	13	13	100.0		38.4	59.9	1.8		17.4
Austria	26,827	21,670	80.8	19.2	12.3	10.2	32.8	25.5	22.7
Belgium	17,396	15,321	88.1	11.9	25.0	12.8	34.9	15.3	21.1
Bosnia and Herzegovina	17,021	16,224	95.3	4.7	42.1	44.9	8.4		16.8
Bulgaria	57,021	49,562	86.9	13.1	31.1	36.0	19.2	0.6	16.8
Croatia	20,886	19,428	93.0	7.0	37.6	36.8	14.6	4.0	16.8
Cyprus	3,697	588	15.9	84.1	15.9				2.9
Czechia	44,784	43,696	97.6	2.4	16.8	16.8	31.8	32.2	25.7
Denmark	25,671	18,304	71.3	28.7	8.0	37.0	24.8	1.5	13.6
Estonia	13,495	7,506	55.6	44.4	31.0	24.6			9.5
Finland	26,472	25,173	95.1	4.9	81.6	13.4			11.7
France	318,886	309,564	97.1	2.9	18.2	22.2	30.6	26.1	24.4
Germany	201,436	185,320	92.0	8.0	12.8	14.0	51.3	13.9	23.9
Greece	42,934	27,680	64.5	35.5	34.6	15.0	12.4	2.5	11.1
Hungary	60,220	45,004	74.7	25.3	33.0	25.4	5.2	11.1	14.9
Iceland	1,909	0	0.0	100.0					0.5
Ireland	43,268	33,903	78.4	21.6	78.3	0.0			9.2
Italy	148,113	123,454	83.4	16.6	29.1	14.3	19.5	20.4	19.3
Latvia	25,046	22,839	91.2	8.8	76.4	14.8			12.6
Liechtenstein	37	37	100.0		77.6	22.4			14.9
Lithuania	37,303	36,000	96.5	3.5	47.4	49.1			15.3
Luxembourg	1,351	1,268	93.8	6.2	26.8	22.3	21.8	23.0	22.3
Malta	44	0	0.0	100.0					0.3
Monaco	0	0	0.0						
Montenegro	2,179	1,786	82.0	18.0	48.8	32.8	0.2	0.2	12.5
Netherlands	22,509	19,704	87.5	12.5	13.1	13.1	35.6	25.7	22.4
North Macedonia	9,146	7,035	76.9	23.1	20.3	47.8	8.8		15.7
Norway	12,593	4,382	34.8	65.2	30.9	3.9			5.5
Poland	181,630	146,666	80.7	19.3	14.4	33.1	28.7	4.5	18.5
Portugal	41,721	28,425	68.1	31.9	21.6	11.5	13.2	21.9	17.1
Romania	133,738	118,059	88.3	11.7	43.8	32.7	11.7	0.0	15.2
San Marino	42	42	100.0		44.9	51.2	3.9		15.8
Serbia (incl. Kosovo)	46,768	37,848	100.0	19.1	28.7	21.9	26.8	3.5	17.1
Slovakia	23,015	18,048	78.4	21.6	63.1	12.6	2.4	0.4	11.4
Slovenia	6,942	6,910	99.5	0.5	1.1	47.5	33.2	17.7	25.1
Spain	237,726	150,683	63.4	36.6	29.2	12.6	13.4	8.2	13.7
Sweden	36,217	10,682	29.5	70.5	20.7	4.5	4.3		4.7
Switzerland	11,359	10,702	94.2	5.8	13.3	26.0	48.5	6.3	23.0
Türkiye	330,826	93,754	28.3	71.7	22.9	3.5	0.7	1.2	6.8
Total	**2,237,952**	**1,664,061**	**74.4**	**25.6**	**26.7**	**18.4**	**19.2**	**10.1**	**16.1**
Total without Türkiye	**1,907,126**	**1,570,307**	**82.3**	**17.7**	**27.3**	**20.9**	**22.4**	**11.7**	**17.7**
EEA-38	**2,237,897**	**1,664,006**	**74.4**	**25.6**	**26.7**	**18.4**	**19.2**	**10.1**	**16.1**
EEA-38 without Türkiye	**1,907,070**	**1,570,252**	**82.3**	**17.7**	**27.3**	**20.9**	**22.4**	**11.7**	**17.7**
EEA-32	**2,155,074**	**1,594,333**	**74.0**	**26.0**	**26.5**	**17.9**	**19.2**	**10.4**	**16.4**
EEA-32 without Türkiye	**1,824,248**	**1,500,579**	**82.3**	**17.7**	**27.2**	**20.5**	**22.5**	**12.0**	**18.1**
EU-27	**1,798,337**	**1,485,458**	**82.6**	**17.4**	**27.3**	**20.6**	**22.5**	**12.2**	**18.2**
Northern Europe	**178,706**	**124,886**	**69.9**	**30.1**	**42.6**	**22.7**	**4.4**	**0.2**	**10.6**
Western Europe	**337,268**	**319,957**	**94.9**	**5.1**	**24.7**	**16.2**	**28.8**	**25.2**	**22.9**
Central Europe	**556,252**	**478,054**	**85.9**	**14.1**	**17.8**	**22.1**	**34.2**	**11.9**	**20.7**
Southern Europe	**540,432**	**390,689**	**72.3**	**27.7**	**28.4**	**15.6**	**16.0**	**12.3**	**16.0**
South-Eastern Europe	**625,294**	**350,476**	**56.0**	**44.0**	**29.6**	**17.3**	**7.8**	**1.3**	**9.9**
	,								
Kosovo	4,167	4,119	98.8	1.2	21.9	37.4	39.5	0.0	21.2
Serbia (without Kosovo)	42,601	33,728	79.2	20.8	29.4	20.3	25.6	3.8	16.7

Note: The percentage value "0.0" indicates that an exposed agricultural area exists, but it is small and estimated to be less than 0.05 %. Empty cells mean no agricultural area in exposure.

Table 3.2 Exposure of crops to O_3 and agricultural area weighted concentrations, O_3 indicator POD_3IAM for crops, 2023

Country	Agricultural area, 2023			Fraction of agricultural area, 2023 (%)					Agricultural-weighted POD_3IAM, 2023
	Total area	> CL for crops (7.9 mmol/m² PLA)		< 7.9	7.9-16	16-24	24-32	> 32	
	(km²)	(km²)	(%)	(mmol/m² PLA)					(mmol/m² PLA)
Albania	7,709	7,611	98.7	1.3	23.1	21.9	25.7	28.0	24.1
Andorra	13	13	100.0		35.5	61.7	2.8		17.4
Austria	26,827	25,743	96.0	4.0	11.2	28.0	41.5	15.3	24.3
Belgium	17,396	16,684	95.9	4.1	4.9	18.7	14.2	58.0	29.3
Bosnia and Herzegovina	17,021	16,893	99.3	0.7	24.1	45.0	29.6	0.5	19.9
Bulgaria	57,021	46,705	81.9	18.1	38.3	27.3	15.4	1.0	14.9
Croatia	20,886	20,784	99.5	0.5	6.3	36.1	46.8	10.3	23.2
Cyprus	3,697	429	11.6	88.4	10.2	1.4			1.7
Czechia	44,784	44,353	99.0	1.0	12.1	13.2	38.1	35.6	27.8
Denmark	25,671	21,127	82.3	17.7	10.9	14.3	43.1	14.1	17.9
Estonia	13,495	7,341	54.4	45.6	19.1	19.7	15.6		11.9
Finland	26,472	25,298	95.6	4.4	68.1	27.4	0.0		13.0
France	318,886	308,121	96.6	3.4	8.1	21.6	28.2	38.7	27.0
Germany	201,436	195,689	97.1	2.9	5.0	11.6	28.7	51.9	28.8
Greece	42,934	30,513	71.1	28.9	37.2	21.8	10.2	1.9	11.3
Hungary	60,220	53,127	88.2	11.8	7.7	26.1	37.1	17.3	22.9
Iceland	1,909	0	0.0	100.0					1.3
Ireland	43,268	41,164	95.1	4.9	82.3	12.8			13.2
Italy	148,113	140,246	94.7	5.3	14.7	22.2	19.6	38.3	25.4
Latvia	25,046	20,481	81.8	18.2	28.3	16.6	36.9		17.4
Liechtenstein	37	37	100.0		77.6	22.4			15.2
Lithuania	37,303	33,141	88.8	11.2	32.8	29.9	26.1		17.4
Luxembourg	1,351	1,268	93.8	6.2	5.5	34.3	12.1	41.8	25.6
Malta	44	0	0.0	100.0					0.0
Monaco	0	0							
Montenegro	2,179	2,167	99.5	0.5	55.3	39.0	5.1	0.1	14.4
Netherlands	22,509	20,801	92.4	7.6	4.9	6.0	16.6	64.9	27.7
North Macedonia	9,146	7,913	86.5	13.5	29.7	47.5	9.3		16.3
Norway	12,593	4,422	35.1	64.9	29.6	5.5			6.1
Poland	181,630	148,591	81.8	18.2	12.5	17.2	44.5	7.6	20.4
Portugal	41,721	30,106	72.2	27.8	19.9	14.6	11.6	26.1	19.5
Romania	133,738	122,363	91.5	8.5	34.3	37.7	18.3	1.2	17.3
San Marino	42	42	100.0			44.9	29.4	25.7	25.2
Serbia (incl. Kosovo)	46,768	43,447	100.0	7.1	5.5	31.6	37.7	18.1	23.9
Slovakia	23,015	23,015	100.0		28.6	40.2	29.8	1.4	20.3
Slovenia	6,942	6,942	100.0		0.6	1.9	37.1	60.4	32.7
Spain	237,726	116,164	48.9	51.1	15.7	10.1	11.3	11.8	12.4
Sweden	36,217	12,751	35.2	64.8	12.7	16.0	3.7	2.8	6.9
Switzerland	11,359	10,556	92.9	7.1	12.3	28.9	50.1	1.7	22.2
Türkiye	330,826	134,577	40.7	59.3	35.9	3.8	0.7	0.2	6.8
Total	**2,237,952**	**1,740,628**	**77.8**	**22.2**	**20.2**	**17.8**	**21.0**	**18.7**	**17.2**
Total without Türkiye	**1,907,126**	**1,606,050**	**84.2**	**15.8**	**17.5**	**20.3**	**24.5**	**21.9**	**19.5**
EEA-38	**2,237,897**	**1,740,572**	**77.8**	**22.2**	**20.2**	**17.8**	**21.0**	**18.7**	**17.2**
EEA-38 without Türkiye	**1,907,070**	**1,605,995**	**84.2**	**15.8**	**17.5**	**20.3**	**24.5**	**21.9**	**19.5**
EEA-32	**2,155,074**	**1,662,541**	**77.1**	**22.9**	**20.4**	**17.2**	**20.6**	**18.9**	**17.2**
EEA-32 without Türkiye	**1,824,248**	**1,527,963**	**83.8**	**16.2**	**17.6**	**19.6**	**24.2**	**22.3**	**19.5**
EU-27	**1,798,337**	**1,512,948**	**84.1**	**15.9**	**17.6**	**19.6**	**24.3**	**22.7**	**19.6**
Northern Europe	**178,706**	**124,562**	**69.7**	**30.3**	**28.6**	**19.8**	**18.8**	**2.6**	**13.2**
Western Europe	**337,268**	**331,122**	**98.2**	**1.8**	**17.4**	**18.7**	**20.1**	**41.9**	**20.4**
Central Europe	**556,252**	**508,054**	**91.3**	**8.7**	**9.7**	**17.3**	**36.7**	**27.6**	**24.7**
Southern Europe	**540,432**	**374,428**	**69.3**	**30.7**	**16.3**	**16.4**	**17.3**	**19.2**	**20.8**
South-Eastern Europe	**625,294**	**402,462**	**64.4**	**35.6**	**32.0**	**18.4**	**11.4**	**2.5**	**12.3**
Kosovo	4,167	4,167	100.0		9.5	42.3	47.4	0.8	23.9
Serbia (without Kosovo)	42,601	39,280	92.2	7.8	5.2	30.5	36.7	19.8	23.7

Note: The percentage value "0.0" indicates that an exposed agricultural area exists, but it is small and estimated to be less than 0.05 %. Empty cells mean no agricultural area in exposure.

Figures 3.1 and 3.2 show the frequency distribution of the agricultural area over some O_3 exposure classes (in terms of POD_3IAM for crops) for each country, for five large European regions, for EU-27, for EEA-32 (with and without Türkiye) and for the total mapping area, for 2022 and 2023. The figures present graphically the core information of Tables 3.1 and 3.2.

Figure 3.1 Percentage of the agricultural area (%) exposed to different values of the indicator POD_3IAM for crops (mmol/m² PLA), 2022

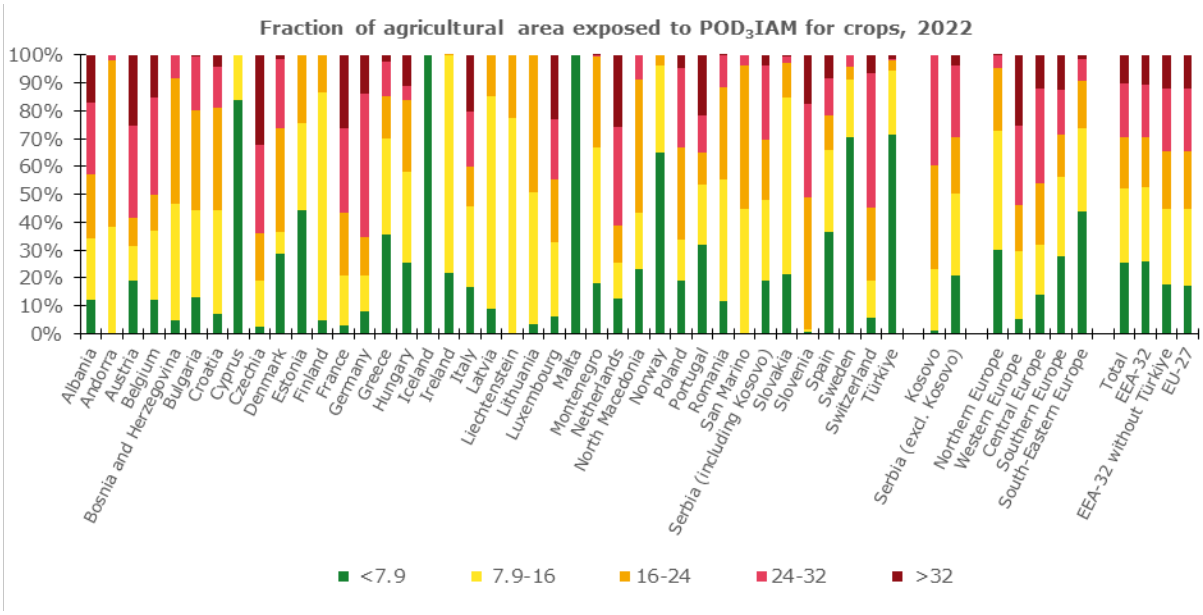

Figure 3.2 Percentage of the agricultural area (%) exposed to different values of the indicator POD_3IAM for crops (mmol/m² PLA), 2023

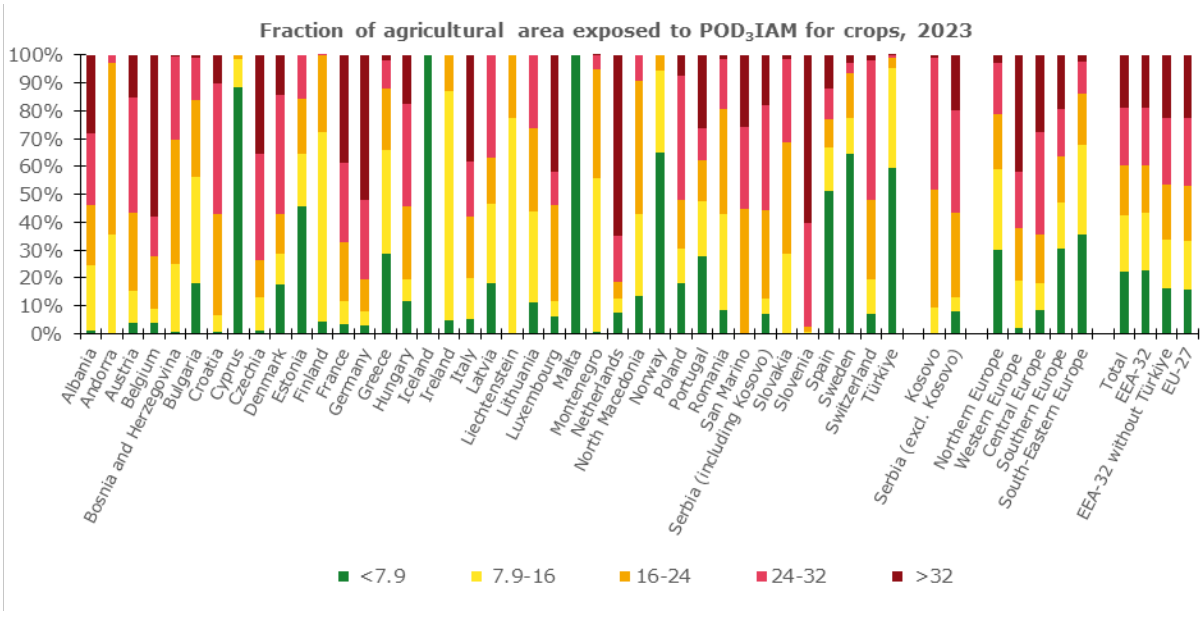

The Figures 3.1 and 3.2 can be used for the new AIR indicator based on the POD_Y. Specifically, the bar showing the frequency distribution for the EEA-32 can be directly used for this purpose.

3.2 Alternative option: Indicator using crop specific metrics POD_6 for wheat and potato

As an alternative option, the indicator using POD_6 for wheat and potato has been prepared. Maps 3.3 and 3.4 present the spatial distribution of POD_6 for wheat and potato in 2022 and 2023, respectively.

Map 3.3 POD_6 for wheat (left) and potato (right), rural map, 2022

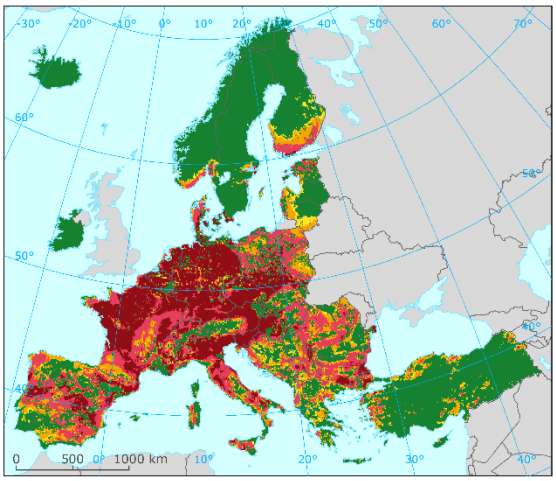

Ozone, POD_6 for wheat Reference Year: 2022
Resolution: 0.1°, transformed to 2 km Rural Map

- 0 - 1.3 mmol/m² PLA
- 1.3 - 1.5 mmol/m² PLA > CL for grain yield
- 1.5 - 2 mmol/m² PLA > CL for 1000-grain weight
- 2 - 3 mmol/m² PLA > CL for protein yield
- 3 - 7 mmol/m² PLA
- non EEA member or cooperating countries

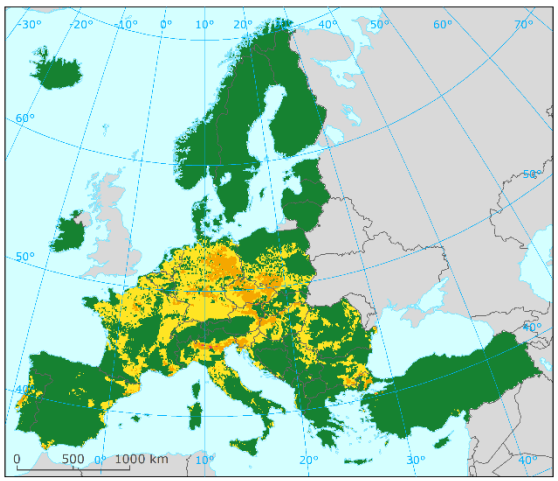

Ozone, POD_6 for potato Reference Year: 2022
Resolution: 0.1°, transformed to 2 km Rural Map

- 0 - 3.8 mmol/m² PLA
- 3.8 - 6 mmol/m² PLA > CL for tuber yield
- 6 - 9 mmol/m² PLA
- 9 - 12 mmol/m² PLA
- 12 - 14 mmol/m² PLA
- non EEA member or cooperating countries

Map 3.4 POD_6 for wheat (left) and potato (right), rural map, 2023

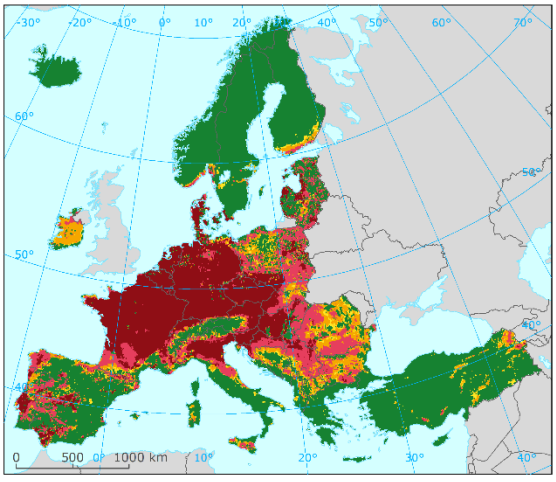

Ozone, POD_6 for wheat Reference Year: 2023
Resolution: 0.1°, transformed to 2 km Rural Map

- 0 - 1.3 mmol/m² PLA
- 1.3 - 1.5 mmol/m² PLA > CL for grain yield
- 1.5 - 2 mmol/m² PLA > CL for 1000-grain weight
- 2 - 3 mmol/m² PLA > CL for protein yield
- 3 - 7 mmol/m² PLA
- non EEA member or cooperating countries

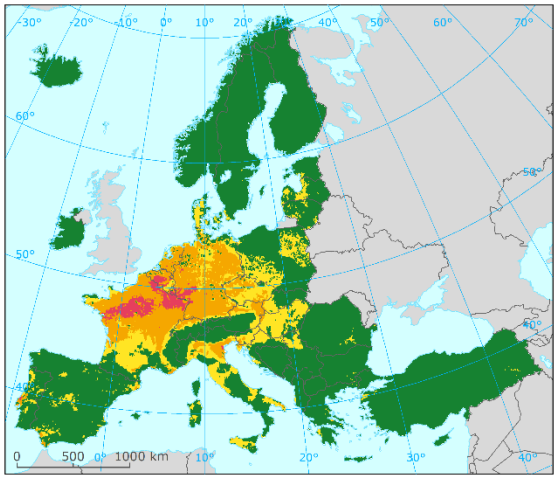

Ozone, POD_6 for potato Reference Year: 2023
Resolution: 0.1°, transformed to 2 km Rural Map

- 0 - 3.8 mmol/m² PLA
- 3.8 - 6 mmol/m² PLA > CL for tuber yield
- 6 - 9 mmol/m² PLA
- 9 - 12 mmol/m² PLA
- 12 - 14 mmol/m² PLA
- non EEA member or cooperating countries

The areas with POD_6 for wheat values below the CL for grain yield (i.e. 1.3 mmol/m^2 PLA) are marked in green. The areas with POD_6 for wheat values in between CL for grain yield and CL for 1,000-grain weight (which is 1.5 mmol/m^2 PLA) and in between CL for 1,000-grain weight and CL for protein yield (which is 2 mmol/m^2 PLA) are marked in yellow and orange, respectively. The areas with POD_6 values for wheat above the CL for protein yield are marked in red and dark red. The areas with POD_6 for potato values below the CL for tuber yield (i.e. 3.8 mmol/m^2 PLA) are marked in green, while the areas with POD_6 for potato values above this threshold are marked in yellow, orange, red and dark red.

In order to estimate the exposure of wheat and potato to O_3 in terms of POD_6 for wheat and potato, respectively, the relevant rural maps of POD_6 have been combined with the area covered by wheat and potato, respectively, according to the agricultural data in 1 km resolution as applied in Schucht et al. (2024). For description of these data, see Annex 2, Section A2.3. Note that the data are less detailed (in terms of spatial resolution) compared to the CLC2018 applied for the basic variant of the new POD_Y-based indicator.

Table 3.3 presents the exposure of wheat and potato to O_3 in terms of POD_6 for wheat and potato, respectively, for the year 2022. The table shows the frequency distribution of the wheat and potato agricultural areas over some exposure classes for EU-27, EEA-32, EEA-38 and the total mapping area (with and without Türkiye in the last three cases) and for five large European regions. In addition, the wheat and potato agricultural area weighted concentrations are presented, i.e. the average values of POD_6 for wheat and potato, respectively, across the relevant agricultural areas. Table 3.4 presents the same numbers for 2023.

Table 3.3 Exposure of wheat (left) and potato (right) to O_3 and agricultural area weighted concentrations, O_3 indicators POD_6 for wheat (left) and potato (right), 2022

Country	Wheat, 2022						Potato, 2022					
	Fraction of wheat agricultural area (%)					Agr.-w. POD_6 wheat	Fraction of potato agricultural area (%)					Agr.-w. POD_6 potato
	< 1.3	1.3-1.5	1.5-2	2-3	> 3		< 3.8	3.8-6	6-9	9-12	> 12	
	(mmol/m² PLA)						(mmol/m² PLA)					
Albania	33.9	13.4	26.4	26.0	0.3	1.49	91.8	7.6	0.7			2.71
Andorra				100		2.50	50.0	50.0				3.55
Austria	18.4	1.2	3.7	11.4	65.3	3.08	38.6	38.5	22.7	0.2		4.09
Belgium	22.6	2.4	4.7	9.4	61.0	2.89	43.0	57.0				3.65
Bosnia and Herzegovina	47.1	18.9	23.1	11.0		1.37	96.9	3.1				2.21
Bulgaria	24.5	3.9	17.3	42.0	12.3	1.97	71.7	25.3	3.0			2.95
Croatia	23.4	11.0	25.3	31.1	9.1	1.84	62.4	37.2	0.4			3.29
Cyprus	90.1	2.5	3.2	4.2		0.41	100					0.13
Czechia	10.5	1.1	3.8	10.8	73.8	3.57	11.4	40.8	47.4	0.5		5.70
Denmark	34.3	3.0	8.8	36.4	17.5	1.81	99.9	0.1				1.49
Estonia	63.5	2.9	8.5	22.3	2.8	1.04	100					1.30
Finland	57.5	6.5	17.1	17.0	1.9	1.34	100					0.61
France	6.2	1.5	8.9	28.9	54.6	2.90	50.5	47.7	1.8	0.0		3.59
Germany	9.8	1.5	3.7	10.8	74.1	3.22	19.6	59.2	21.2			4.85
Greece	60.0	11.4	18.0	9.9	0.6	1.12	96.1	3.2	0.8			1.48
Hungary	30.7	1.8	6.6	28.6	32.3	2.18	39.6	47.8	12.6			3.67
Iceland	100					0.01	100					0.01
Ireland	100					0.33	100					0.24
Italy	22.9	3.1	11.8	31.1	31.0	2.40	65.2	27.1	7.3	0.4		3.10
Latvia	79.1	9.5	8.8	2.5	0.1	0.89	100					1.08
Liechtenstein		37.8	5.4	51.4	5.4	1.93	100					1.03
Lithuania	52.1	23.3	22.0	2.6		1.27	100					1.70
Luxembourg	30.7	0.5	2.3	19.5	47.0	2.47	46.0	54.0				3.68
Malta							100					0.0
Monaco												
Montenegro	59.8	10.7	15.0	14.5		1.15	98.9	1.1				1.75
Netherlands	14.6	1.4	5.7	10.7	67.6	3.19	37.1	62.9				3.79
North Macedonia	71.6	9.0	10.4	9.0	0.0	1.07	99.9	0.1				1.87
Norway	73.8		25.0	1.3		0.67	100					0.27
Poland	26.4	2.7	15.7	35.7	19.5	1.99	65.0	28.9	6.1			3.11
Portugal	37.3	6.2	15.3	26.3	15.0	1.66	81.9	13.3	4.8			2.15
Romania	32.6	6.1	22.0	37.6	1.7	1.59	68.5	31.4	0.1			2.91
San Marino				100		2.53	75.7	24.3				3.33
Serbia (incl. Kosovo)	28.4	8.6	26.7	31.5	4.8	1.64	77.1	22.9	0.0			2.65
Slovakia	55.5	6.0	15.5	16.6	6.5	1.27	64.4	32.1	3.4	0.0		3.01
Slovenia	1.6		0.8	22.4	75.2	3.52	8.4	66.0	25.7			5.39
Spain	32.5	4.9	16.1	32.3	14.2	1.78	93.3	5.9	0.7			1.70
Sweden	88.5	1.6	4.6	2.6	2.7	0.35	100					0.25
Switzerland	6.6	1.2	5.7	46.4	40.1	2.73	47.9	51.9	0.1			3.34
Türkiye	84.1	4.2	7.3	3.5	0.9	0.59	98.5	0.9	0.7	0.0		0.91
Total	**39.2**	**4.4**	**11.7**	**21.1**	**23.7**	**1.84**	**71.6**	**23.5**	**4.9**	**0.0**		**2.53**
Total without Türkiye	**31.0**	**4.4**	**12.5**	**24.3**	**27.8**	**2.07**	**66.7**	**27.5**	**5.7**	**0.0**		**2.82**
EEA-38	**39.2**	**4.4**	**11.7**	**21.1**	**23.7**	**1.84**	**71.6**	**23.5**	**4.9**	**0.0**		**2.53**
EEA-38 without Türkiye	**31.0**	**4.4**	**12.5**	**24.3**	**27.8**	**2.07**	**66.7**	**27.5**	**5.7**	**0.0**		**2.82**
EEA-32	**39.1**	**4.0**	**11.2**	**21.0**	**24.7**	**1.86**	**70.8**	**24.0**	**5.2**	**0.0**		**2.53**
EEA-32 without Türkiye	**30.5**	**4.0**	**11.9**	**24.4**	**29.2**	**2.11**	**65.6**	**28.4**	**6.0**	**0.0**		**2.84**
EU-27	**30.6**	**4.0**	**11.9**	**24.3**	**29.2**	**2.10**	**65.7**	**28.2**	**6.1**	**0.1**		**2.84**
Northern Europe	**67.8**	**7.1**	**11.6**	**10.6**	**2.9**	**0.98**	**100.0**	**0.0**				**0.82**
Western Europe	**13.1**	**1.2**	**5.4**	**21.6**	**58.8**	**2.87**	**48.2**	**50.6**	**1.2**			**3.48**
Central Europe	**20.1**	**2.1**	**8.7**	**22.2**	**46.9**	**2.62**	**39.4**	**44.1**	**16.4**	**0.1**		**4.08**
Southern Europe	**30.9**	**4.8**	**15.2**	**30.1**	**19.0**	**1.94**	**81.9**	**14.9**	**3.1**	**0.1**		**2.27**
South-Eastern Europe	**60.1**	**6.0**	**14.1**	**17.2**	**2.6**	**1.08**	**87.5**	**11.8**	**0.7**	**0.0**		**1.78**
Kosovo	16.1	20.2	41.5	21.2	0.9	1.69	5.2					2.87
Serbia (without Kosovo)	30.1	7.0	24.7	32.9	5.3	1.63	25.3	0.0				2.62

Note: The percentage value "0.0" indicates that an exposed agricultural area exists, but it is small and estimated to be less than 0.05 %. Empty cells mean no agricultural area in exposure.

Table 3.4 Exposure of wheat (left) and potato (right) to O_3 and agricultural area weighted concentrations, O_3 indicators POD_6 for wheat (left) and potato (right), 2023

Country	Wheat, 2023						Potato, 2023					
	Fraction of wheat agricultural area (%)					Agr.-w. POD_6 wheat	Fraction of potato agricultural area (%)					Agr.-w. POD_6 potato
	< 1.3	1.3-1.5	1.5-2	2-3	> 3		< 3.8	3.8-6	6-9	9-12	> 12	
	(mmol/m² PLA)						(mmol/m² PLA)					
Albania	76.3	9.0	12.3	2.3		0.90	95.7	4.3				1.63
Andorra				100		2.13	100					1.39
Austria	5.9	0.9	2.4	7.3	83.6	4.00	23.8	40.3	35.8			4.83
Belgium	3.0	0.2	0.2	1.7	94.8	4.42	4.3	15.8	49.9	30.0		7.66
Bosnia and Herzegovina	50.1	11.5	26.2	12.3		1.31	100					1.35
Bulgaria	22.6	5.8	36.6	34.2	0.9	1.67	99.5	0.5				1.82
Croatia	18.6	0.8	4.7	43.4	32.4	2.46	52.0	46.6	1.4			3.71
Cyprus	98.7	1.3				0.10	100					0.14
Czechia	1.0	0.2	0.2	2.4	96.2	4.33	4.7	57.4	37.9			5.69
Denmark	29.4	1.4	2.7	7.3	59.2	2.68	54.1	44.6	1.3			3.08
Estonia	63.9	1.6	4.4	23.5	6.6	1.05	97.0	3.0				1.84
Finland	84.3	3.6	7.8	4.4		0.86	100					1.29
France	6.6	1.3	3.1	11.6	77.5	3.76	15.1	23.1	46.0	15.8		6.50
Germany	4.6	0.8	2.0	5.7	86.9	4.16	8.7	17.5	70.0	3.7		6.56
Greece	99.2	0.5	0.1	0.2	0.0	0.44	96.2	3.7	0.2			1.58
Hungary	11.4	0.9	1.5	31.2	54.9	2.88	23.1	74.4	2.6			4.11
Iceland	100					0.06	100					0.00
Ireland	27.4	5.3	56.3	11.0		1.46	100					1.80
Italy	51.1	4.2	6.9	15.7	22.1	1.75	53.3	36.1	10.3	0.2		3.60
Latvia	50.7	2.3	4.1	20.4	22.5	1.47	75.8	24.2				2.55
Liechtenstein	37.8	5.4	45.9	2.7	8.1	1.58	91.9	8.1				2.09
Lithuania	48.8	4.2	11.3	24.9	10.7	1.43	87.3	12.7				2.80
Luxembourg	3.1			2.4	94.5	5.14	5.5	6.8	42.5	45.2		8.03
Malta							100					0.00
Monaco												
Montenegro	58.4	9.4	17.8	14.4		1.15	100					0.66
Netherlands	6.4	0.4	1.2	3.6	88.4	3.95	11.7	10.9	76.3	1.1		6.93
North Macedonia	42.9	15.2	31.6	10.3		1.36	100.0					1.38
Norway	83.8	7.5	6.3	2.5		0.63	100.0					0.58
Poland	24.7	4.4	14.7	41.1	15.0	2.00	69.7	30.0	0.3			3.04
Portugal	35.1	3.6	13.4	30.7	17.1	1.81	77.4	16.6	5.2	0.8		2.23
Romania	14.5	10.7	35.3	39.2	0.4	1.82	97.7	2.3				2.28
San Marino		21.6	73.0	5.4		1.65	100.0					2.92
Serbia (incl. Kosovo)	9.8	3.7	14.9	57.1	14.6	1.94	83.1	16.9				2.44
Slovakia	5.3	3.2	14.8	40.8	35.8	2.70	63.9	32.4	3.7			3.13
Slovenia	1.6		0.6	5.5	92.3	3.85	16.7	72.0	11.3			4.76
Spain	68.1	2.7	6.5	16.1	6.6	0.92	93.3	5.9	0.8			1.22
Sweden	90.2	3.1	3.4	1.4	2.0	0.29	98.3	1.5	0.2			0.47
Switzerland	11.2	1.9	5.2	9.6	72.1	3.84	32.2	29.5	38.3	0.0		4.51
Türkiye	93.2	2.7	3.2	0.9	0.0	0.52	99.6	0.4				0.86
Total	**42.9**	**3.2**	**8.8**	**16.1**	**29.0**	**1.98**	**65.8**	**16.6**	**15.0**	**2.6**		**3.12**
Total without Türkiye	**33.8**	**3.3**	**9.8**	**18.9**	**34.3**	**2.25**	**59.7**	**19.5**	**17.7**	**3.1**		**3.53**
EEA-38	**42.9**	**3.2**	**8.8**	**16.1**	**29.0**	**1.98**	**65.8**	**16.6**	**15.0**	**2.6**		**3.12**
EEA-38 without Türkiye	**33.8**	**3.3**	**9.8**	**18.9**	**34.3**	**2.25**	**59.7**	**19.5**	**17.7**	**3.1**		**3.53**
EEA-32	**43.4**	**3.0**	**8.3**	**15.3**	**30.0**	**2.02**	**64.6**	**17.0**	**15.7**	**2.8**		**3.18**
EEA-32 without Türkiye	**33.8**	**3.0**	**9.3**	**18.1**	**35.8**	**2.31**	**57.9**	**20.1**	**18.6**	**3.3**		**3.62**
EU-27	**33.9**	**3.0**	**9.3**	**18.2**	**35.6**	**2.30**	**58.1**	**20.1**	**18.5**	**3.3**		**3.62**
Northern Europe	**71.5**	**3.0**	**5.8**	**9.8**	**9.8**	**0.99**	**91.1**	**8.8**	**0.1**			1.57
Western Europe	**3.6**	**0.7**	**5.2**	**3.8**	**86.8**	**4.05**	**12.0**	**13.8**	**55.3**	**18.9**		7.06
Central Europe	**12.0**	**2.1**	**6.8**	**21.8**	**57.3**	**3.23**	**34.0**	**34.0**	**30.7**	**1.3**		4.74
Southern Europe	**57.7**	**3.2**	**7.1**	**18.5**	**13.6**	**1.34**	**75.5**	**20.3**	**4.1**	**0.1**		2.27
South-Eastern Europe	**60.4**	**5.2**	**14.6**	**17.4**	**2.5**	**1.12**	**96.1**	**3.8**	**0.1**			1.47
Kosovo	19.0	7.0	25.9	47.5	0.7	2.32	100					1.58
Serbia (without Kosovo)	8.5	3.3	13.4	58.3	16.5	1.89	80.8	19.2				2.55

Note: The percentage value "0.0" indicates that an exposed agricultural area exists, but it is small and estimated to be less than 0.05 %. Empty cells mean no agricultural area in exposure.

Figures 3.3 and 3.4 show the frequency distribution of the wheat and potato agricultural area over some O_3 exposure classes (in terms of POD_6 for wheat and potato) for each country, for five large European regions, for EU-27, for EEA-32 (with and without Türkiye) and for the total mapping area, for years 2022 and 2023. The figures present graphically the core information of Tables 3.3 and 3.4.

Figure 3.3 Percentage of the wheat and potato agricultural area (%) exposed to different values of the indicator POD_6 for wheat (above) and POD_6 for potato (below) (mmol/m^2 PLA), 2022

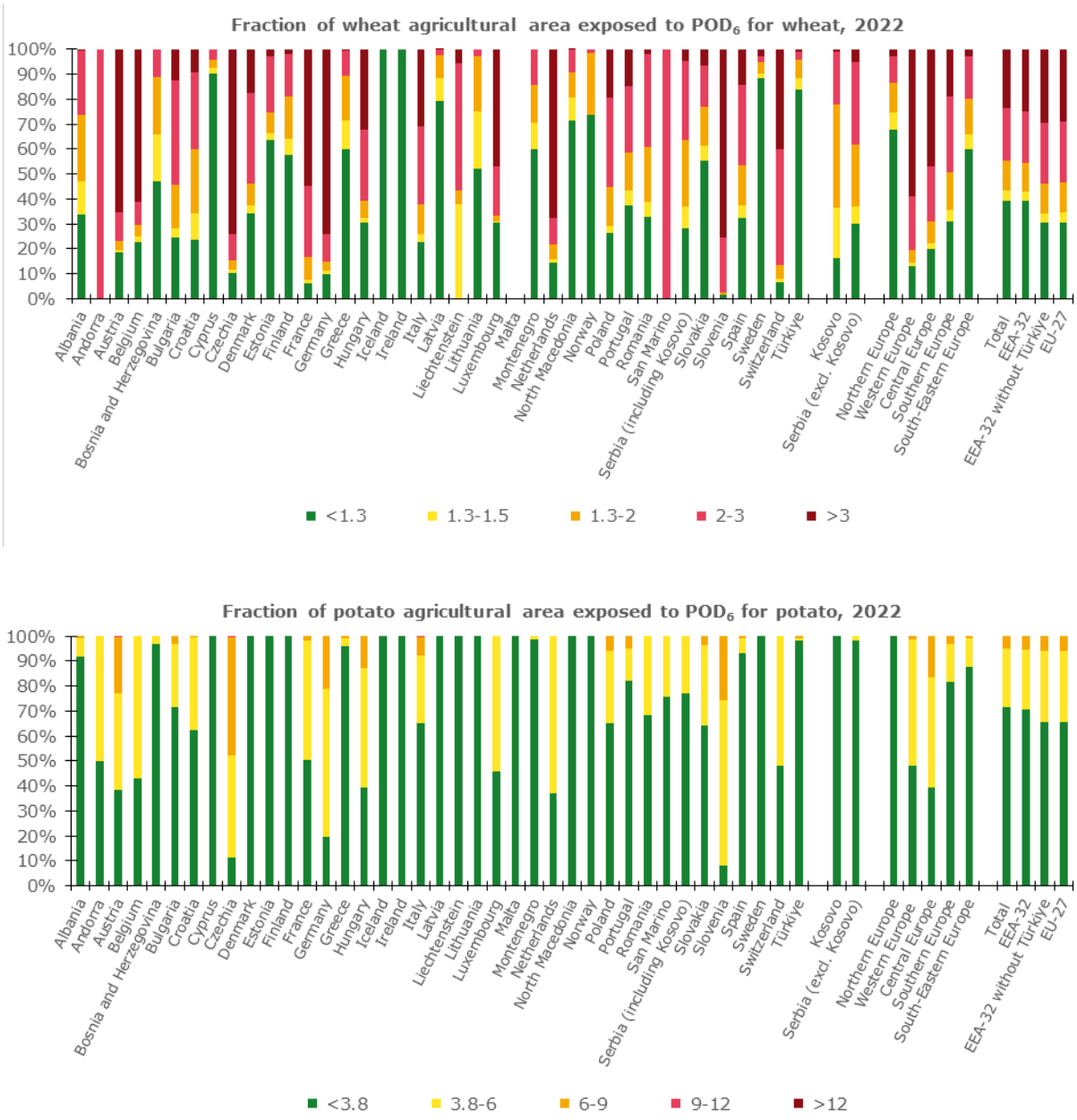

Figure 3.4 Percentage of the wheat and potato agricultural area (%) exposed to different values of the indicator POD_6 for wheat (above) and POD_6 for potato (below) (mmol/m² PLA), 2023

4 Comparison of the new indicator based on POD_Y and the current AIR004 indicator based on AOT40 results

In this chapter, the results of the new indicator based on POD_Y are compared with the current AIR004 indicator based on the AOT40 metric. In addition, the basic and alternative variants of the new POD_Y-based indicator are mutually compared, and also the wheat and potato parts of the alternative POD_Y-based indicator.

Figure 4.1 presents the scatter plots showing the correlation between the agricultural area weighted values of (i) POD_Y in different variants and (ii) AOT40 for vegetation, as calculated for individual countries, both for 2022 and 2023.

Figure 4.1 Correlation between agricultural area weighted values of POD_3IAM for crops (left), POD_6 for wheat (middle) and POD_6 for potato (right) (y-axis) versus agricultural area weighted values of AOT40 for vegetation (x-axis) per country for years 2022 (above) and 2023 (below)

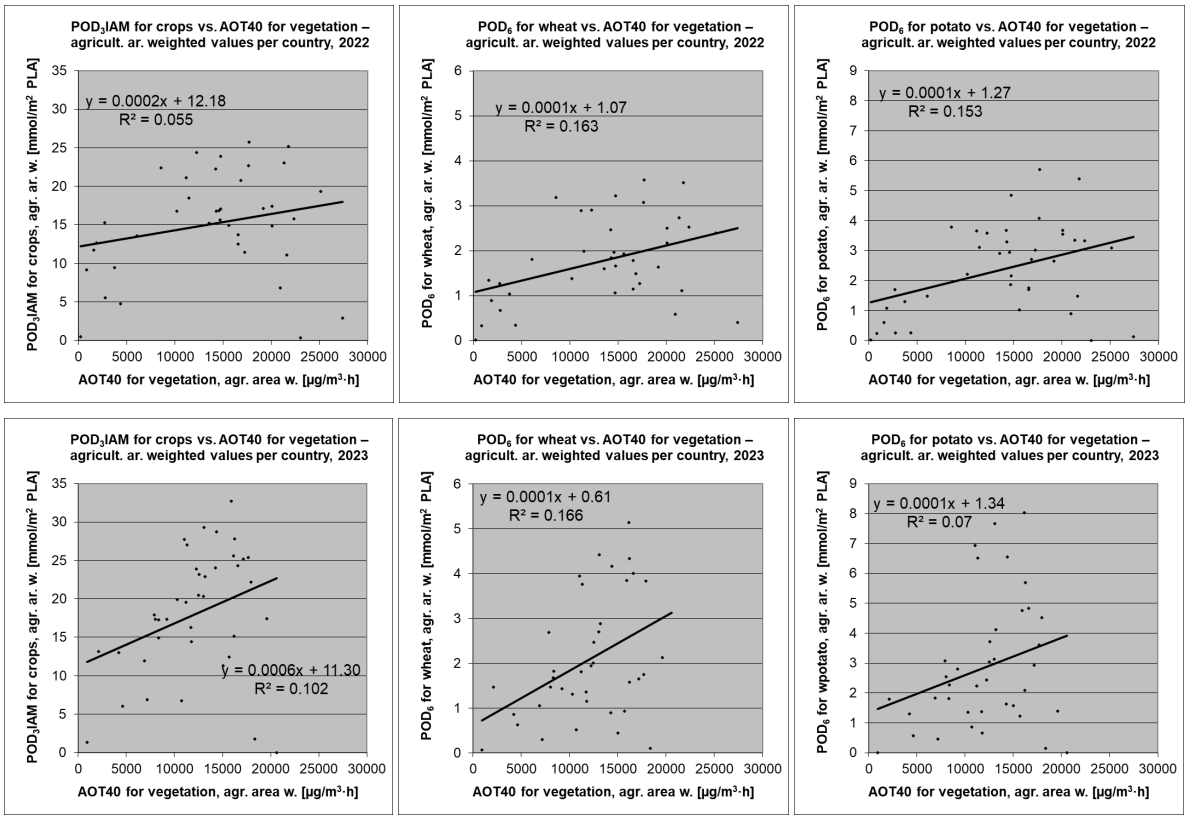

Looking at the results, one can see quite a poor correlation between the weighted values of POD_Y (for all variants) and AOT40 for vegetation.

Figure 4.2 presents the scatter plots showing the correlation between the agricultural area weighted values of (i) POD_6 for wheat or potato and (ii) POD_3IAM for crops, and also between (i) POD_6 for potato and (ii) POD_6 for wheat, as calculated for individual countries. The correlation shows the level of relationship between two parameters, i.e. the level of interchangeability of these parameters.

The results show stronger correlation between the weighted values of the three different variants of POD_Y, compared to the correlation between the weighted values of POD_Y and AOT40 (as shown in Figure 4.1).

Figure 4.2 Correlation between agricultural area weighted values of POD_6 for wheat (left) and POD_6 for potato (middle and right) (y-axis) versus agricultural area weighted values of POD_3IAM for crops (left and middle) and POD_6 for wheat (right) (x-axis) per country for years 2022 (above) and 2023 (below)

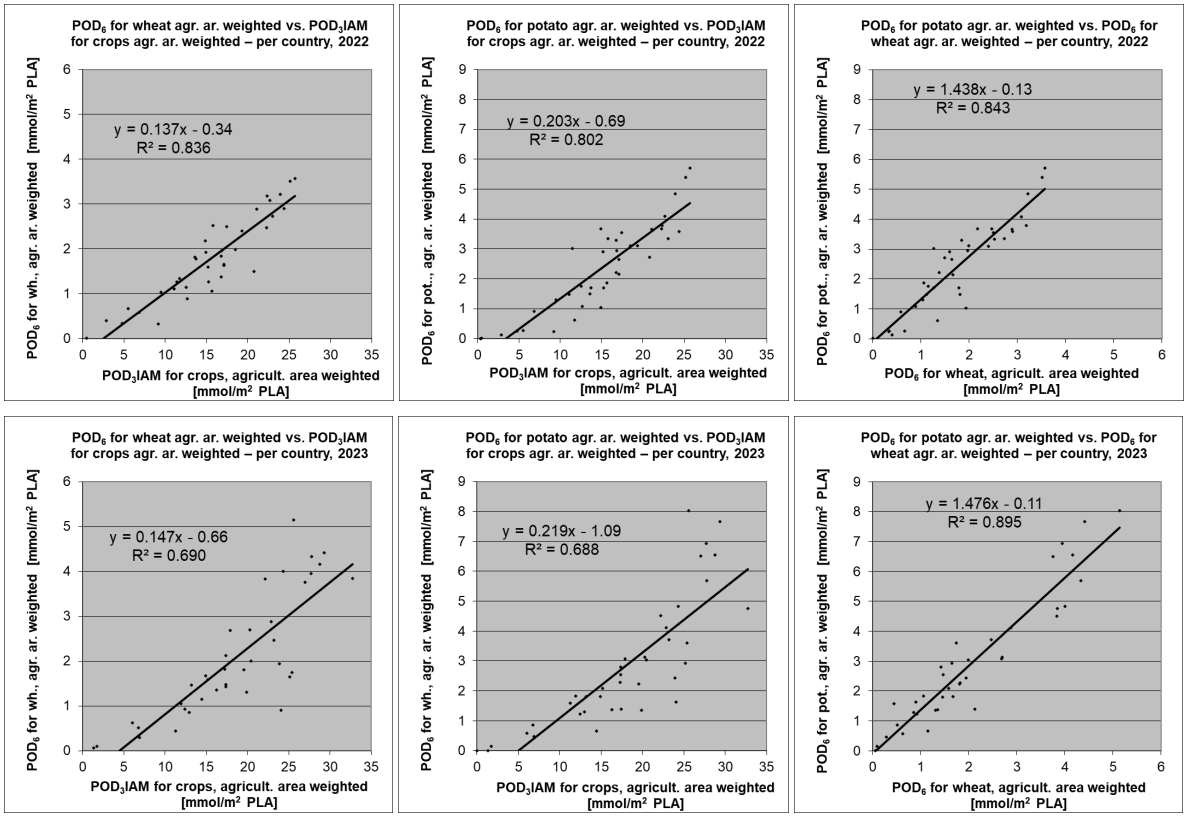

Map 4.1 presents inter-annual differences for AOT40 for vegetation (as used for the current AIR004 indicator) and for the three different variants of POD_Y (as applied for the new POD_Y-based indicator, either in the basic or the alternative variants).

One can see that the inter-annual differences of AOT40 for vegetation show different patterns compared to the inter-annual differences of the three POD_Y variants. On the other hand, the inter-annual difference of the three POD_Y variants shows quite similar patterns (despite some differences).

Huge differences in both spatial distribution and inter-annual variability between AOT40 and POD_Y metrics are in agreement with the well-known facts, already mentioned before, that high ambient O_3 concentrations do not lead to high O_3 fluxes when stomata are closed during unfavourable environmental conditions and that, conversely, quite low O_3 concentrations can still lead to fairly high O_3 fluxes when stomata are open under favourable environmental conditions. Another reason for the different spatial and temporal distributions of AOT40 and POD_Y might be that the AOT40 gives more weight to peak ozone concentrations due to the cut-off at 80 µg/m^3 (i.e. 40 ppb), while the POD_Y indicators are more sensitive to variations of background O_3 levels.

Map 4.1 Difference in concentrations between 2022 and 2023 for ozone indicators AOT40 for vegetation (upper left), POD_3IAM for crops (upper right), POD_6 for wheat (bottom left) and POD_6 for potato (bottom right)

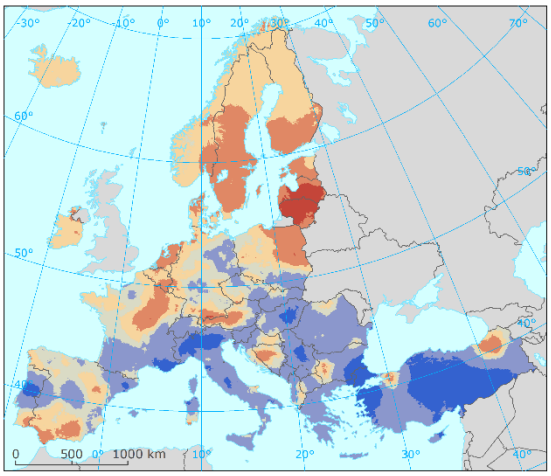

Ozone, AOT40 for Vegetation
Interannual Difference between 2023 and 2022

Difference: 2023 - 2022
Resolution: 2 km

Rural Map

- ≤ - 6 000 µg/m³·h
- - 6 000 – - 2 000 µg/m³·h
- - 2 000 – 0 µg/m³·h
- 0 – 2 000 µg/m³·h
- 2 000 – 6 000 µg/m³·h
- > 6 000 µg/m³·h
- no available data
- unmapped countries

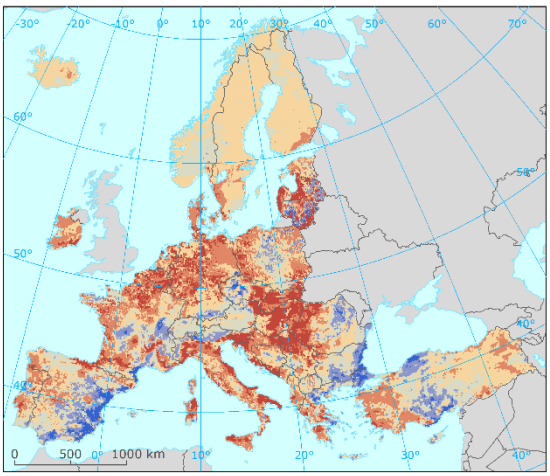

Ozone, POD_3IAM for crops
Interannual Difference between 2023 and 2022

Difference: 2023 - 2022
Resolution: 0.1°, transformed to 2 km

Rural Map

- ≤ 8 mmol/m² PLA
- -8 – -3 mmol/m² PLA
- -3 – 0 mmol/m² PLA
- 0 – 3 mmol/m² PLA
- 3 – 8 mmol/m² PLA
- > 8 mmol/m² PLA
- no available data
- unmapped countries

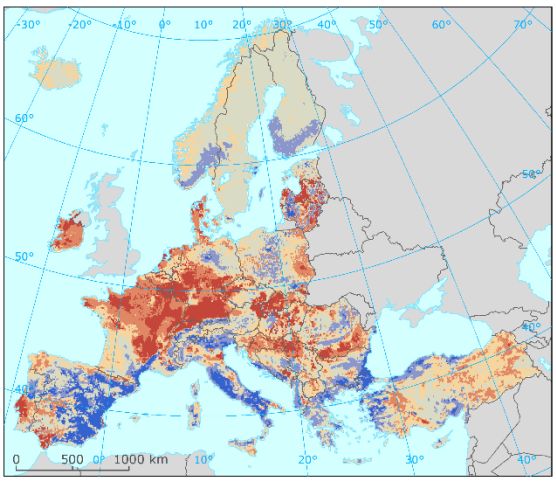

Ozone, POD_6 for wheat
Interannual Difference between 2023 and 2022

Difference: 2023 - 2022
Resolution: 0.1°, transformed to 2 km

Rural Map

- ≤ -1.5 mmol/m² PLA
- -1.5 – -0.6 mmol/m² PLA
- -0.6 – 0 mmol/m² PLA
- 0 – 0.6 mmol/m² PLA
- 0.6 – 1.5 mmol/m² PLA
- > 1.5 mmol/m² PLA
- no available data
- unmapped countries

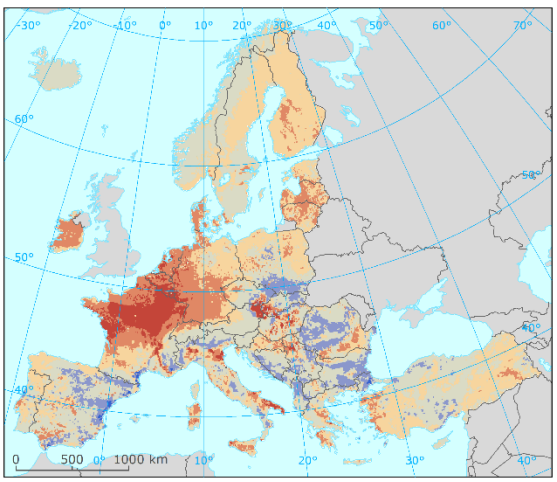

Ozone, POD_6 for potato
Interannual Difference between 2023 and 2022

Difference: 2023 - 2022
Resolution: 0.1°, transformed to 2 km

Rural Map

- ≤ -4 mmol/m² PLA
- -4 – -1.5 mmol/m² PLA
- -1.5 – 0 mmol/m² PLA
- 0 – 1.5 mmol/m² PLA
- 1.5 – 4 mmol/m² PLA
- > 4 mmol/m² PLA
- no available data
- unmapped countries

Based on the results of both the correlation scatterplots and the inter-annual difference maps, it is concluded that the new AIR indicator based on POD_Y should complement the current AIR004 indicator, not substitute it, in order to ensure a more comprehensive risk analysis based on current knowledge. Apart from that, as all variants of POD_Y show similarities, it is concluded that the new indicator based on the POD_3IAM for crops can be fairly used to represent different crop species at regional to continental scales, which is relevant for the European-wide POD_Y-based indicator, with species-specific POD_Y estimates more suitable for more specific risk assessments, in agreement with the CLRTAP methodology.

Adopting a dual approach based on AOT40 (exposure) and POD_Y (dose) is therefore not a duplication but a logical step to improve the assessment of the O_3 burden and the associated risk of negative effects on vegetation. While the environmental exposure expressed by AOT40 allows relatively simple monitoring of air quality and long-term exposure trends, the absorbed dose expressed by POD_Y is a metric with biological relevance capable of explaining damage to crops and ecosystems. Particularly, the use of both metrics should be recommended for areas where asynchrony between plant physiological activity and high O_3 concentrations due to weather conditions or climate change is suspected. Keeping both complementary metrics would ensure a better estimation of risks.

5 Discussion of the reasons for POD_Y levels and inter-annual variability

POD_Y is a multifactorial indicator influenced by both atmospheric O_3 concentration and physiological activity of the target vegetation. It is the accumulated stomatal O_3 flux (F_{sto}) above a threshold of Y during a specified time or growth period (for its calculation, see Annex 1, Eq. A1.5). The hourly stomatal O_3 flux is calculated using the O_3 concentration at the top of the canopy, the stomatal conductance (g_{sto}) and the quasi-laminar and the leaf surface resistances (see Annex 1, Eq. A1.3). The O_3 concentration at the canopy top is calculated using the ambient O_3 concentration and different resistances (see Annex 1, Eq. A1.1), while the stomatal conductance is calculated using the species-specific maximum stomatal conductance and six limitation functions (see Annex 1, Eq. A1.2). As a result, the POD_Y levels and their inter-annual variability are difficult to interpret without disentangling the respective contributions of each limiting function to the actual absorbed O_3 flux. This chapter presents an analysis of the contributions of each limitation function to the POD_Y and their inter-annual variation between 2022 and 2023. The analysis has been performed for POD_6 for wheat for 2022 and 2023 (see Map 3.3 left and Map 3.4 left). The main reason for selecting this POD_Y variant was that the maps of the POD_6 for wheat has been created under the ETC HE since 2018, so that the ETC HE has more experience with this indicator, compared to the POD_3IAM for crops. This chapter plays a role as a case study, as it aims to analyse the inter-annual POD_Y differences (which was not done so far under the ETC HE). Apart from that, due to the similarities between POD_6 for wheat and POD_3IAM for crops (see Chapter 4), some of its results might be applicable to POD_3IAM for crops as well.

To evaluate the physiological limitations affecting O_3 uptake in European wheat crops, a relative indicator was constructed based on a data-driven modelling framework. This indicator allows to quantify how much each physiological function reduces the potential O_3 flux, offering a meaningful and interpretable perspective on the stomatal limitation landscape across biogeographical regions or countries. Based on this, the main parameters that influence the POD_Y levels can be seen, next to the O_3 concentrations.

The input data for calculating this indicator consist of hourly values for the following physiological limitation functions for wheat that have been used in the computation of the POD_6 for wheat:

- f_{phen} (phenology),
- f_{O3} (O_3 response),
- f_{light} (light),
- f_{temp} (temperature),
- f_{VPD} (vapour pressure deficit),
- f_{SMI} (soil moisture index)

These values have been spatially aggregated over biogeographical regions or countries for a full growing season (e.g. a unique value of each function for each region/country at each hour of the growing period for the years 2022 and 2023 is obtained by averaging values of all grid cells of the relevant region or country) making it possible to recompute an aggregated POD_Y that is called POD_Y of reference (POD_Y_ref). However, the spatial aggregation has an effect on the recalculation of this POD_Y_ref. Indeed, the recomputed F_{sto} does not exceed the 6 nmol/m^2 PLA per second threshold as often as when calculated at 2 km resolution. The reason is that the limitation functions as well as the O_3 concentration are smoothed by the spatial aggregation. As a consequence, the accumulation of POD_6_ref account for just a few hours (when F_{sto} exceed 6 nmol/m^2 PLA per second) in the whole year, which is not enough to be used for an analysis of the contribution of the limitation functions. Therefore, the threshold of 3 nmol/m^2 PLA per second for F_{sto} is preferred to the classical threshold of 6 nmol/m^2 PLA per second allowing a larger temporal cover to be used for this sensitivity analysis. So, the POD_Y_ref indicator is called POD_3_ref in order to take into account this threshold value.

5.1 Methodology: Definition of the relative Indicator

For each limitation function f, the following values have been computed:

- The reference cumulative O_3 flux (POD_3_ref) using all the limiting functions aggregated over biogeographical regions or countries. (For biogeographical regions, see Annex 1, Map A1.1.)
- A modified O_3 flux (POD_3_without_f) by **setting function f to 1 wherever its original value was non-zero**, keeping other functions unchanged. (meaning that function f has no effect on the total flux POD_3_without_f)

The indicator "Contribution_f" is then defined as:

$$\text{Contribution}_f = \frac{\text{POD}_3\text{\_without\_f} - \text{POD}_3\text{\_ref}}{\text{POD}_3\text{\_without\_f}} * 100 \qquad (5.1)$$

This represents the percentage of the O_3 flux lost specifically due to function f, relative to the potential flux without its limitation. Therefore, it is an indicator of the effectiveness of the limitation: "how much of the potential POD_3_without_f has been limited by this function?"

The advantage of the indicator it that it offers an independent measure for each function, without interference from others. It can be used on either bioregion-aggregated data or country-level data without changing methodology. It will allow the identification of the dominant limiting functions in each region or country but also the assessment of how physiological stresses differ between years (e.g. 2022 vs 2023). However, considering that the effectiveness of the limitation is related to each POD_3_without_f, the sum of the effectiveness of the limitation for all function is not 100%.

To validate the approach, it is necessary to check that the POD_3_ref calculated from aggregated data over biogeographical regions or countries is well correlated with the original POD_6 for wheat values which were computed at grid cell level and then aggregated to the biogeographical regions / countries. The analysis of the different POD calculation shows a correlation which is quite high for the inter-annual differences, (R^2 = 0.74 for countries, R^2 = 0.89 for biogeographical regions), see Figure 5.1. Thus, the results of the analysis for the recomputed POD_3 can be applied for explaining the inter-annual differences of the original POD_6 for wheat.

Figure 5.1 Correlation between POD_3_ref for wheat calculated based on spatially aggregated limiting functions (y-axis) versus spatial average of POD_6 for wheat (calculated at 2 km resolution) (x-axis) for aggregations over countries (left) and biogeographical regions (right), inter-annual difference 2023-2022

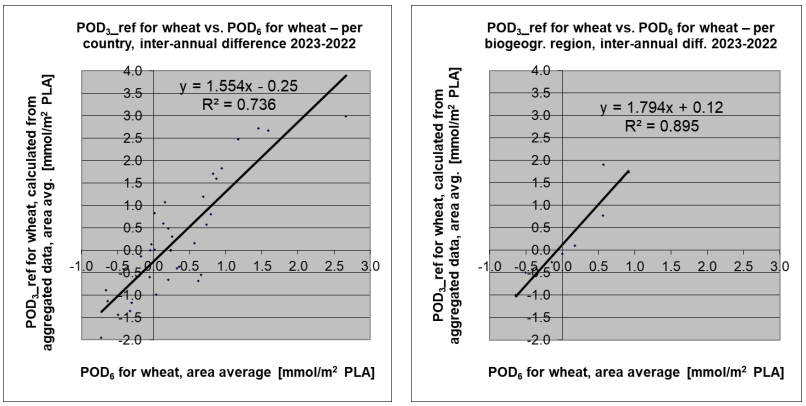

5.2 Results

The results from this analysis are presented with:

- Inter-annual differences in POD_3_ref (2023-2022) at country level (Figure 5.2) and biogeographical region level (Annex 3, Figure A3.1 left).
- Inter-annual differences in the efficiency of the reduction of POD_3_ref for f_{phen}, f_{temp}, f_{SMI}, f_{VPD} (2023-2022) at country level (Figure 5.3, Figure 5.4, Figure 5.5 and Figure 5.6, since those functions are the most limiting ones of the six considered functions) and biogeographical region level (Annex 3, Figure A3.1 right).
- Heatmaps of POD_3_ref and heatmaps of the different contributions of the functions for years 2022 and 2023 (Figure 5.7 and Figure 5.8 for aggregation at the country level and Annex 3, Figure A3.2 and Figure A3.3 for aggregation at the level of biogeographical regions).

Figure 5.2 POD_3_ref for wheat inter-annual variation: 2023-2022, country level, in mmol/m² PLA

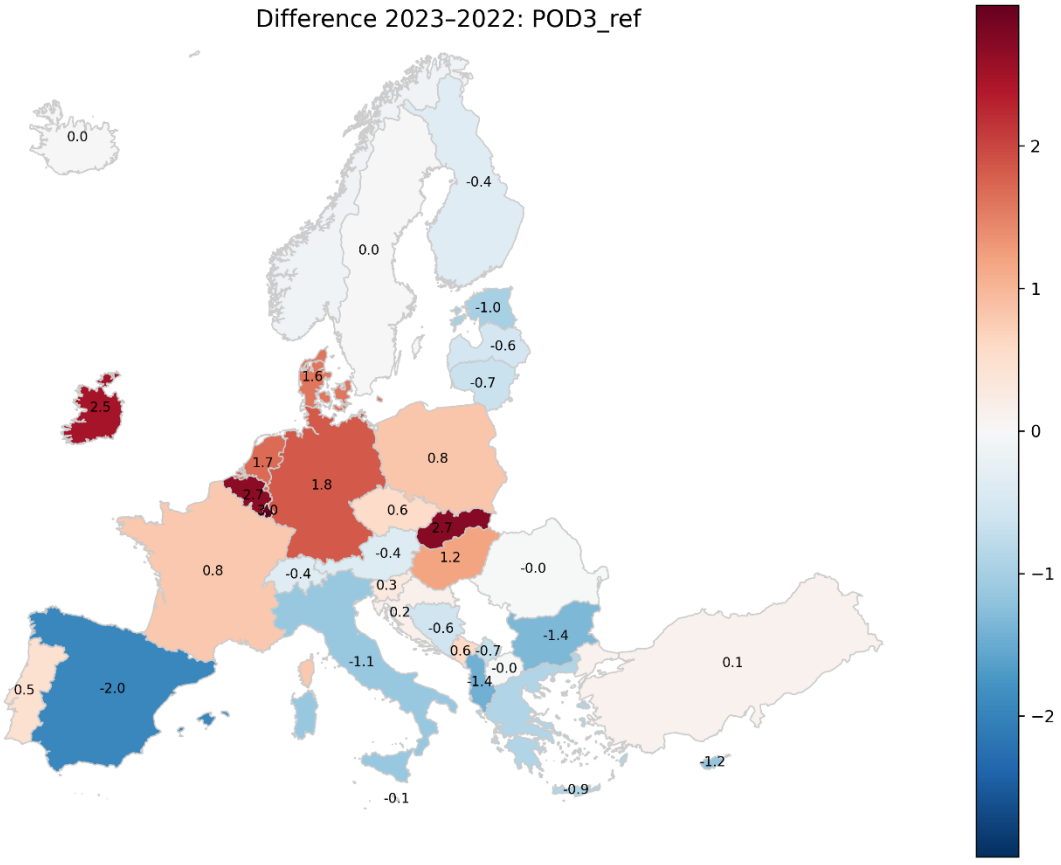

Figure 5.3 Inter-annual variation 2023-2022 for the efficiency of reduction of POD_3_ref for wheat for f_{phen} (phenology) at country level (in percentage points)

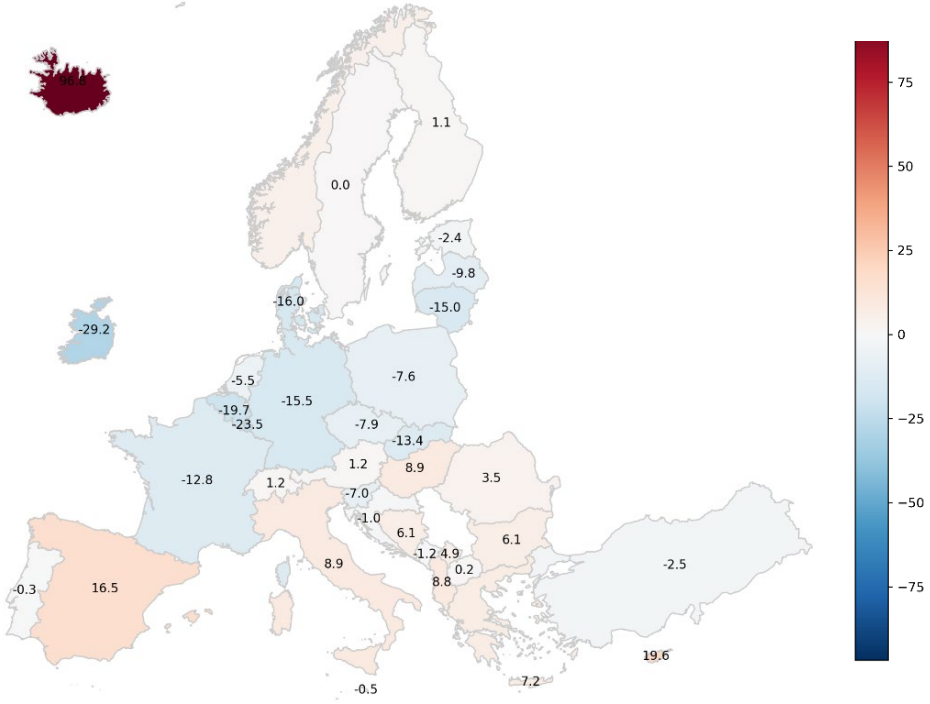

Figure 5.4 Inter-annual variation 2023-2022 for the efficiency of reduction of POD_3_ref for wheat for f_{temp} (temperature) at country level (in percentage points)

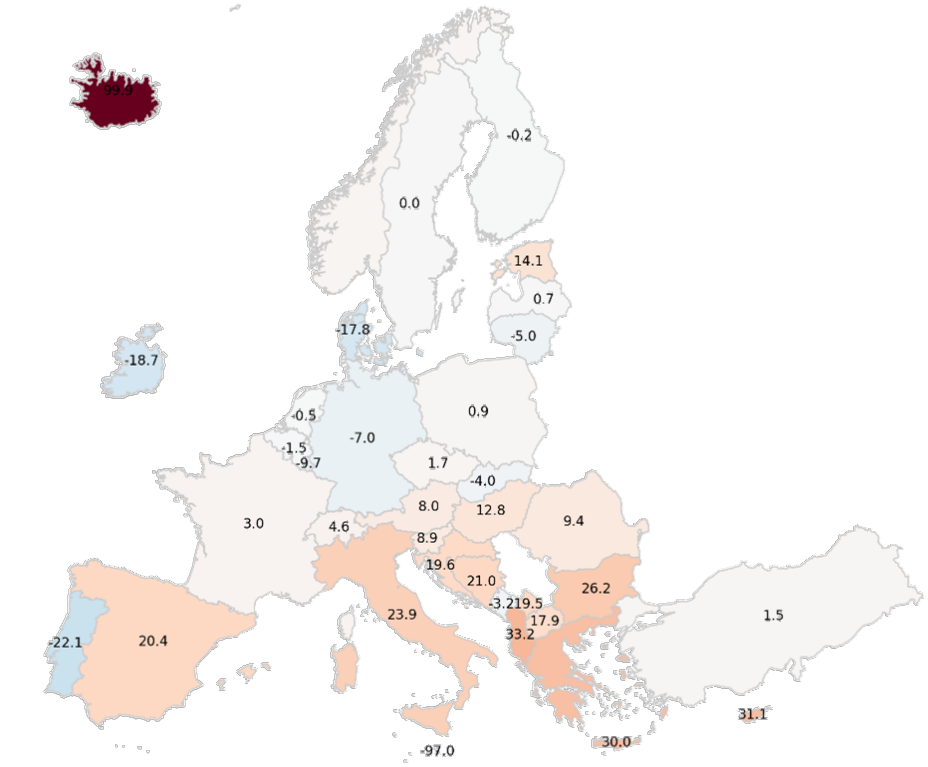

Figure 5.5 Inter-annual variation 2023-2022 for the efficiency of reduction of POD_3_ref for wheat for f_{SMI} (soil moisture index) at country level (in percentage points)

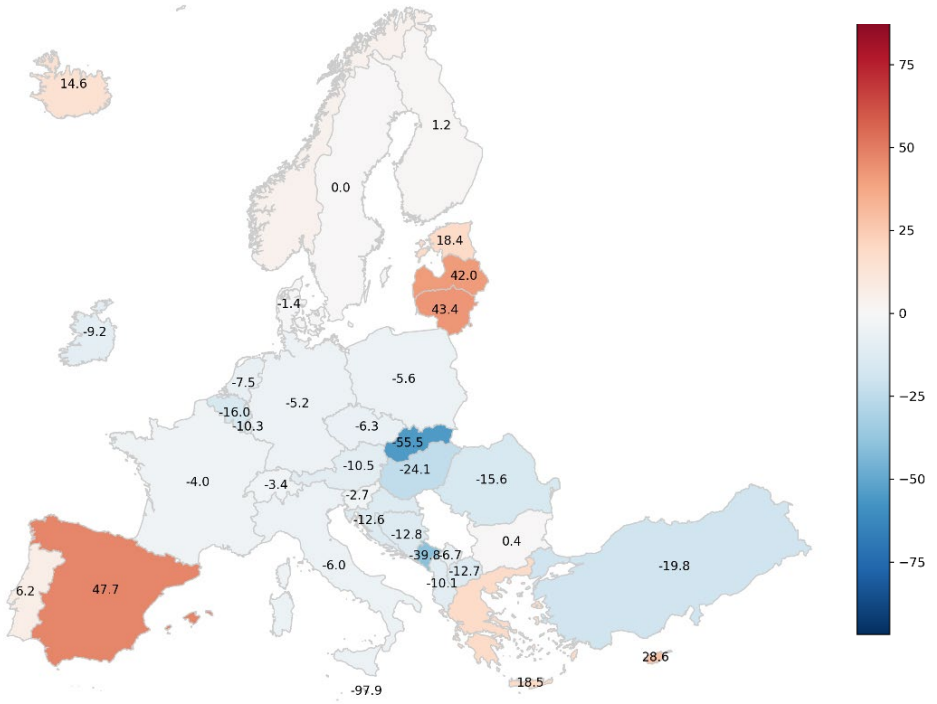

Figure 5.6 Inter-annual variation 2023-2022 for the efficiency of reduction of POD_3_ref for wheat for f_{VPD} (vapour pressure deficit) at country level (in percentage points)

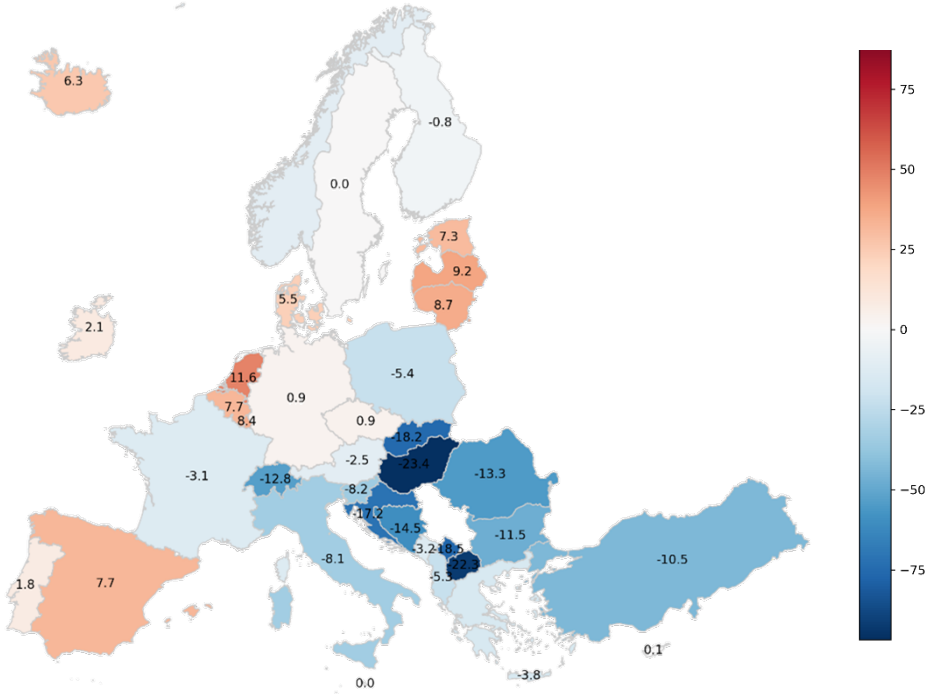

Figure 5.7 POD_3_ref for wheat in mmol/m² PLA (left) and efficiency of the limitation functions for its reduction in % (right) in 2022 for countries

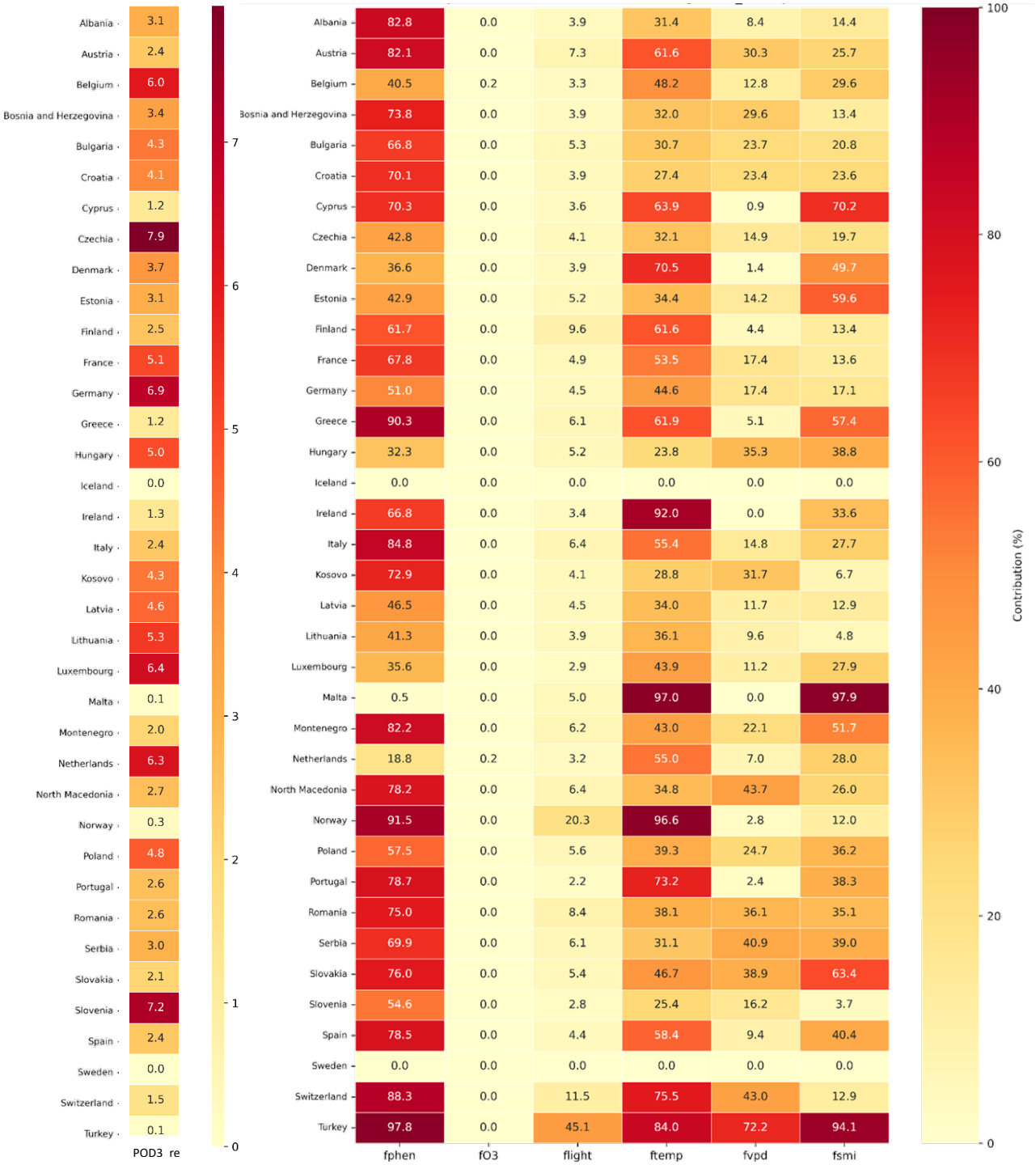

Figure 5.8 POD_3_ref for wheat in mmol/m² PLA (left) and efficiency of the limitation functions for its reduction in % (right) and in 2023 for countries

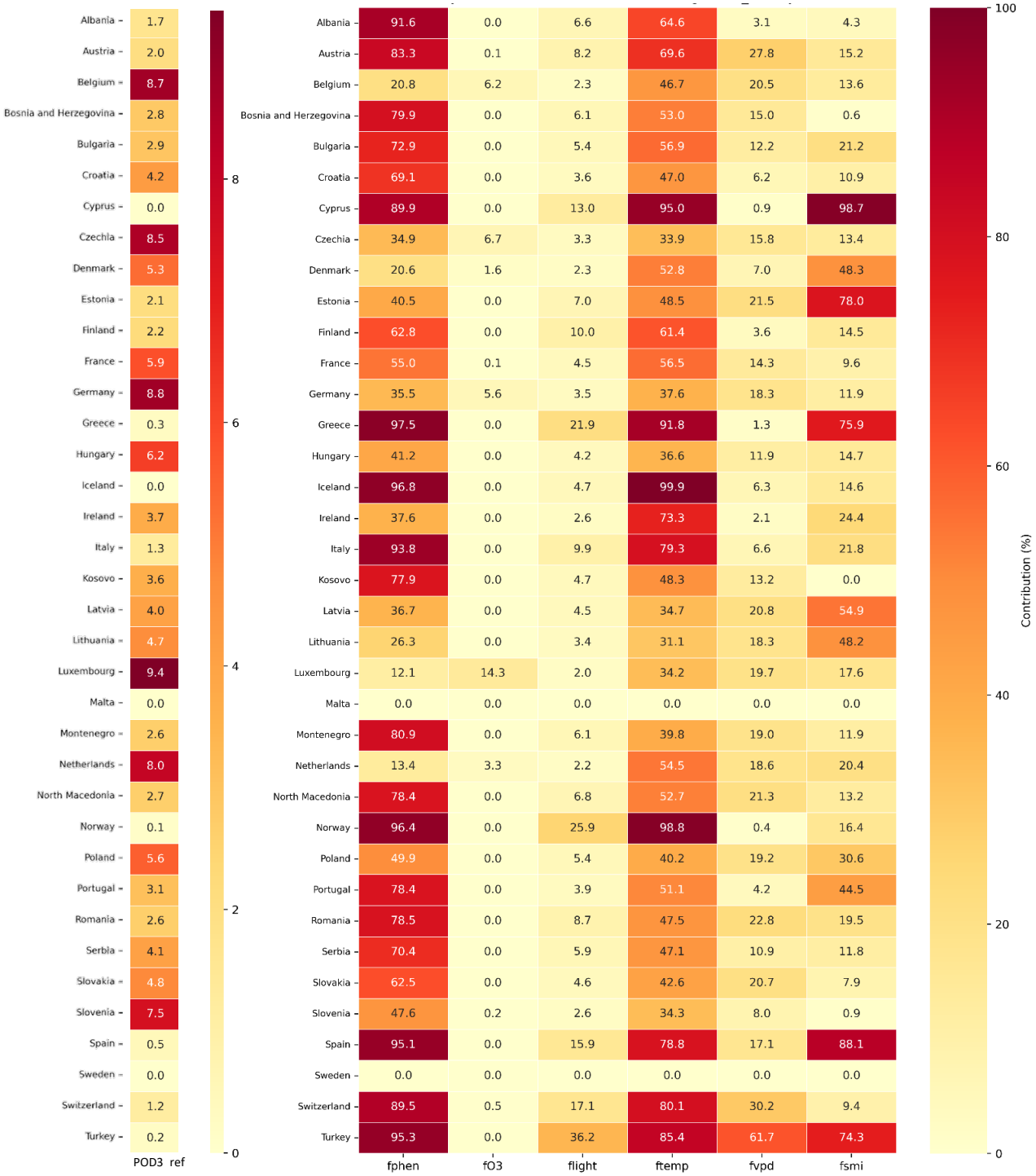

Looking at the POD_3_ref development between 2022 and 2023 for aggregation at country level (Figure 5.2), it shows that the Northern countries (Finland, Baltic countries), some countries around Mediterranean (Spain, Albania, Cyprus, Italy, Greece, Bosnia and Herzegovina, Kosovo), Bulgaria and some Alpine countries (Austria, Switzerland) have an aggregated POD_3_ref higher in 2022 than 2023. For other countries, mostly in the western and central Europe (Luxembourg, Belgium, Slovakia, Ireland, Germany, Netherlands, Hungary, France, Poland, Czechia, Slovenia, Portugal), a POD_3_ref increase from 2022 to 2023 is seen. Focusing at biogeographical regions level (Annex 3, Figure A3.1), one can see the highest POD_3_ref increases for Continental, Atlantic, Pannonian and Steppic biogeographical regions, while the steepest decrease for the Mediterranean biogeographical region.

Regarding the POD_3_ref results at country level for the efficiency of reduction (Figure 5.7 and Figure 5.8), **f_{phen}, f_{temp} and to a lesser extent f_{SMI} seems to be the major restrictive functions for POD_3_ref** in a lot of countries for both year 2022 and 2023. **f_{VPD}** is never the highest restrictive function.

Regarding the biogeographical regions (Annex 3, Figures A3.2 and A3.3): For 2022, the main efficiency reduction is for f_{phen} for all regions except Atlantic and Artic regions (for which the highest is f_{temp}), which is mostly followed by f_{temp}. f_{SMI} remains high in Anatolian, Boreal and Alpine regions. For 2023, the main efficiency reduction come also from f_{phen} for all regions except Atlantic and Artic regions (f_{temp}), followed mostly by f_{temp}. f_{SMI} remains high in Boreal, Anatolian and Mediterranean regions.

In the end, one can say:

- two limitation functions play a **major role**: **f_{phen}** and **f_{temp}**
- **f_{SMI} is a bit less restrictive followed by f_{VPD}** very often less restrictive
- **f_{O3} is almost never restrictive** because it always has greater value than f_{phen}
- **behaviour** of limitation functions are not the same between countries (or biogeographical regions)
- **inter-annual variation of the POD_3** is due to the combination of the restrictiveness of **f_{phen}, f_{temp}, f_{SMI}** and **f_{VPD}** and depends also on the level of the O_3 concentration. The analysis shows that there is no general pattern in the behaviour of the limitation functions that may explain this inter-annual variation between 2022 and 2023.
- These results reflect the inter-annual variability in O_3 concentration and growing conditions, showing that a two year long period is not long enough to extract meaningful conclusions about trends in O_3 effect risks. However, this exercise is useful to understand the level of temporal and geographical variability of the POD_Y.

6 Conclusions and recommendations

This report proposes a new indicator based on POD_Y as complementary information to the current EEA indicator *AIR004 – Exposure of Europe´s ecosystem to ozone*, which consists of two parts related to the agricultural and forested areas. Similarly to the AIR004, the new POD_Y-based indicator should also show the O_3 exposure of crops and forests separately. This report develops the first part of the new indicator, which is related to the flux-related O_3 exposure of crops. The flux-related O_3 exposure of forest trees is suggested to be developed in 2026.

Two options of the new indicator related to the crops are considered, i.e. the crop specific POD_Y indicator and a more generic metric based on the POD_Y used in the Integrated Assessment Modelling (i.e. POD_YIAM), which can be applied for different crops. The advantage of the crop specific POD_Y metric is in its more exact estimation of the O_3 impacts on the corresponding crop, however, it should be applied only to areas covered by this specific crop. On the other hand, the POD_YIAM is more suitable for estimating the O_3 impacts on the wide variety of crops, and thus it can be applied to areas covered by crops in general. For this reason, the metric POD_3IAM for crops is recommended to be used in the POD_Y-based indicator for crops.

In the report, the POD_3IAM for crops has been applied as a basic option for this new indicator. Its results for 2022 and 2023 have been calculated and analysed. Additionally, as an alternative option, also the crop specific metrics POD_6 for wheat and potato have been applied. Subsequently, the results of the new indicator based on the POD_3IAM for crops metrics have been compared with the current AIR004 indicator based on the AOT40 for vegetation metric. In addition, the basic and alternative options of the new POD_Y-based indicator have also been mutually compared. Based on the results of both the correlation scatterplots and the inter-annual difference maps, it has been concluded that the new AIR indicator based on POD_Y should complement the current AIR004 indicator rather than substitute it, in order to ensure a more comprehensive risk analysis based on current knowledge. Apart from that, it has been concluded that the new indicator based on the POD_3IAM for crops can be fairly used to represent different crop species.

In the report, the POD_3IAM for crops indicator have been applied for the same agricultural areas as for which is applied the current AIR004 indicator (i.e. for CLC level-1 class No. 2 “Agricultural areas”). However, its applicability also for pastures that are included in these agricultural areas (i.e. for CLC level-2 class No. 2.3) should be examined in the future, i.e. whether the use of risk indicators specific for pastures does not lead into a considerable change in areas under the risk of O_3 negative effects.

The results support the view that AOT40 and POD_Y should be considered as complementary indicators (or environmental policy tools). While the AOT40 is more relevant for exposure analysis and air quality trends, the POD_Y represents a more effects-oriented indicator for vegetation because it reflects the O_3 dose actually absorbed by plants. The combination of both approaches provides a more comprehensive picture of the exposure to O_3 and the associated risk of effects on European vegetation.

Adopting a dual approach based on AOT40 (exposure) and POD_Y (dose) is therefore not a duplication but a logical step to improve the assessment of the O_3 burden and the associated risk of negative effects on vegetation. While the environmental exposure expressed by AOT40 allows relatively simple monitoring of air quality and long-term exposure trends, the absorbed dose expressed by POD_Y is a metric with biological relevance capable of explaining damage to crops and ecosystems. It is therefore recommended that both AOT40- and POD_Y-based indicators continue to be analysed and reported in the long term, in order to enable to identify trends in the risk of negative effects.

At the same time, the AOT40 is currently the only O_3 indicator included in the Ambient Air Quality Directive (EU, 2024) for the protection of vegetation and next to this, its levels can be simply calculated

based on the O_3 monitoring data. Therefore, it should further continue to be applied. Its complementary use with more biologically meaningful and effects-oriented indicators for vegetation protection like POD_Y should be promoted. However, at the same time, one should bear in mind that in contrast to the AOT40, the POD_Y calculation is quite complex and the POD_Y values are highly sensitive to the setting of different parameters used in their calculation.

POD_Y is a complex indicator, which depends on different variables. High ambient O_3 concentrations do not necessarily lead to high POD_Y values, e.g., if stomata are closed during unfavourable environmental conditions. Conversely, quite low O_3 concentrations can still lead to fairly high O_3 fluxes (and POD_Y values) when stomata are open under favourable environmental conditions. For that reason, the POD_Y levels and inter-annual differences are in general difficult to be understood. Thus, in addition to the development and testing of the new POD_Y-based air indicator, the reasons for the POD_Y levels and inter-annual differences have been analysed and discussed in the report for POD_Y for wheat, as a case study. It seems that phenology and temperature and also soil moisture in water-limited regions play a major role in the POD_Y levels, apart from the O_3 concentrations.

As a follow-up of this report, it is recommended for the next period to develop also the second part of the POD_Y-based indicator, i.e. the one related to forest trees.

List of abbreviations

Abbreviation	Name	Reference
AOT40	Accumulated Ozone exposure over a Threshold of 40 ppb (i.e. 80 µg/m³) in a specific period	https://eur-lex.europa.eu/legal-content/EN/TXT/?uri=CELEX:32024L2881
AQ	Air quality	
CLC	Corine Land Cover	https://land.copernicus.eu/pan-european/corine-land-cover
CLRTAP	Convention on Long-range Transboundary Air Pollution (Air Convention)	https://unece.org/environment-policy/air
EEA	European Environment Agency	www.eea.europa.eu
EEA-32	the 32 EEA member countries (EU-27 + Iceland, Liechtenstein, Norway, Switzerland and Turkey)	https://www.eea.europa.eu/help/glossary/eea-glossary/eea-32
EEA-38	the 38 EEA member and cooperating countries (EEA-32 plus Albania, Bosnia and Herzegovina, Kosovo under UN Security Council Resolution 1244/99, Montenegro, North Macedonia and Serbia)	https://www.eea.europa.eu/en/about/working-practices/docs-register/eea-writing-manual
EMEP	The co-operative programme for monitoring and evaluation of the long-range transmission of air pollutants in Europe	https://www.emep.int
EIONET	European Environment Information and Observation Network	https://www.eionet.europa.eu/
ETC HE	European Topic Centre on Human Health and the Environment	https://www.eionet.europa.eu/etcs
EU-27	the 27 EU Member States (as of 1 February 2020)	https://www.eea.europa.eu/en/about/working-practices/docs-register/eea-writing-manual
IAM	Integrated Assessment Modelling	
ICP Vegetation	International Cooperative Programme on Effects of Air Pollution on Natural Vegetation and Crops	https://icpvegetation.ceh.ac.uk/
NILU	Norwegian Institute for Air Research	https://www.nilu.no/
PLA	Projected Leaf Area	https://icpvegetation.ceh.ac.uk/chapter-3-mapping-critical-levels-vegetation
POD_Y	Phytotoxic Ozone Dose above a threshold of Y nmol/m² PLA per second	https://icpvegetation.ceh.ac.uk/chapter-3-mapping-critical-levels-vegetation
POD_YIAM	POD_Y for a vegetation type for application in large-scale modelling such as integrated assessment modelling (POD_YIAM), accumulated over a stated time period during daylight hours.	https://icpvegetation.ceh.ac.uk/chapter-3-mapping-critical-levels-vegetation
POD_YSPEC	POD_Y for a specific plant species or group of plant species (POD_YSPEC), accumulated over a stated time period during daylight hours.	https://icpvegetation.ceh.ac.uk/chapter-3-mapping-critical-levels-vegetation
VOCs	volatile organic compounds	

References

Agathokleous, E., et al., 2020, 'Ozone affects plant, insect, and soil microbial communities: A threat to terrestrial ecosystems and biodiversity', *Science Advances* 6, pp. 1-17 (https://doi.org/10.1126/sciadv.abc1176) accessed 24 April 2025.

Agyei, T., et al., 2020, 'The impact of drought on total ozone flux in a mountain Norway spruce forest', *Journal of Forest Science* 66, pp. 280-278 (https://doi.org/10.17221/129/2019-JFS) accessed 24 April 2025.

Ainsworth, E. A., 2016, 'Understanding and improving global crop response to ozone pollution', *The Plant Journal* 90, pp. 886-897 (https://doi.org/10.1111/tpj.13298) accessed 24 April 2025.

Anav, A., et al., 2016, 'Comparing concentration-based (AOT40) and stomatal uptake (PODY) metrics for ozone risk assessment to European forests', *Global Change Biology* 22, pp. 1608-1627 (https://doi.org/10.1111/gcb.13138) accessed 24 April 2025.

Ashmore, M. R., 2003, '*Surface ozone effects on vegetation*', in: Holton, J. R., Curry, J. A., Pyle, J. A. (eds.), Encyclopedia of Atmospheric Sciences, Elsevier Science Ltd., London, pp. 1663-1671.

Ashmore, M. R., 2005, 'Assessing the future global impacts of ozone on vegetation', *Plant, Cell and Environment* 28, pp. 949-964 (https://doi.org/10.1111/j.1365-3040.2005.01341.x) accessed 24 April 2025.

Ashmore, M., et al., 2004, 'New directions: a new generation of ozone critical levels for the protection of vegetation in Europe', *Atmospheric Environment* 38, pp. 2213-2214 (https://doi.org/10.1016/j.atmosenv.2004.02.029) accessed 24 April 2025.

CAMS, 2024, *CAMS European air quality forecasts, ENSEMBLE data. Copernicus Atmosphere Monitoring Service (CAMS) Atmosphere Data Store (ADS)* (https://ads.atmosphere.copernicus.eu/datasets/cams-europe-air-quality-forecasts?tab=overview) accessed on 21 October 2024.

Cieslik, S., 2009, 'Ozone fluxes over various plant ecosystems in Italy: a review', *Environmental Pollution* 157, pp. 1487-1496 (https://doi.org/10.1016/j.envpol.2008.09.050) accessed 24 April 2025.

CLRTAP, 2024, Manual on Methodologies and Criteria for Modelling and Mapping Critical Loads and Levels and Air Pollution Effects, Risks, and Trends. Update 2024. Chapter III: "Mapping Critical levels for Vegetation and Lichens", UNECE Convention on Long-range Transboundary Air Pollution (https://www.umweltbundesamt.de/sites/default/files/medien/11850/publikationen/123_2024_texte_manual_on_methodologies_and_criteria.pdf) accessed 24 April 2025.

CLRTAP, 2017, *Scientific Background Document A of Chapter 3 of "Manual on methodologies and criteria for modelling and mapping critical loads and levels of air pollution effects, risks and trends"* (https://icpvegetation.ceh.ac.uk/sites/default/files/ScientificBackgroundDocumentAOct2018.pdf) accessed 24 April 2025.

CLRTAP, 2020, *Scientific Background Document B of Chapter 3 of "Manual on methodologies and criteria for modelling and mapping critical loads and levels of air pollution effects, risks and trends"*

(https://icpvegetation.ceh.ac.uk/sites/default/files/Scientific%20Background%20document%20B%20June%202020.pdf) accessed 11 December 2020.

Coates, J., et al., 2016, The influence of temperature on ozone production under varying NO_x conditions – a modelling study ', *Atmospheric Chemistry and Physics* 16, pp. 11601-11615 (https://doi.org/10.5194/acp-16-11601-2016) accessed 24 April 2025.

Colette, A., et al., 2018, *Long term evolution of the impacts of ozone air pollution on agricultural yields in Europe. A modelling analysis for the 1990-2010 period*, Eionet Report ETC/ACM 2018/15 (https://www.eionet.europa.eu/etcs/etc-atni/products/etc-atni-reports/eionet_rep_etcacm_2018_15_o3impacttrends) accessed 26 August 2020.

Cox, W.M. and Chu, S., 1993, 'Meteorologically adjusted ozone trends in urban areas: A probabilistic approach', *Atmospheric Environment Part B* 27, pp. 425-434 (https://doi.org/10.1016/0957-1272(93)90019-3) accessed 24 April 2025.

Cressie, N., 1993, *Statistics for spatial data,* Wiley series, New York.

Danielson, J. J. and Gesch, D. B., 2011, *Global multi-resolution terrain elevation data 2010 (GMTED2010)*, U.S. Geological Survey Open-File Report, pp. 2011-1073 (https://pubs.er.usgs.gov/publication/ofr20111073) accessed 19 November 2020.

Defra, 2024, *UK Air information resource, Data archive*, UK Department for Environment Food & Rural Affairs (https://uk-air.defra.gov.uk/data/). Data extracted in April 2024.

Defra, 2025, *UK Air information resource, Data archive*, UK Department for Environment Food & Rural Affairs (https://uk-air.defra.gov.uk/data/). Data extracted in March 2025.

Deumier, J. M. and Hannon, C., 2010, 'La période d' initiation de la tubérisation: comment la repérer?' (in French), CNIPT (http://www.cnipt.fr/wp-content/uploads/2013/10/Irrigation-juin-2010.pdf) accessed 8 February 2021.

EEA, 2016, *Biogeographical regions in Europe* (http://www.eea.europa.eu/data-and-maps/data/biogeographical-regions-europe-3) accessed 26 September 2022.

EEA, 2020, *Air quality in Europe – 2020 report, EEA Report No 9/2020, European Environment Agency* (https://www.eea.europa.eu/publications/air-quality-in-europe-2020-report) accessed 24 April 2025.

EEA, 2024, *Air Quality e-Reporting. Air quality database* (https://www.eea.europa.eu/data-and-maps/data/aqereporting-8). Data extracted in March 2024.

EEA, 2025a, *Air Quality e-Reporting. Air quality database* (https://www.eea.europa.eu/data-and-maps/data/aqereporting-8). Data extracted in February 2025.

EEA, 2025b, *Exposure of Europe's ecosystems to ozone* (https://www.eea.europa.eu/ims/exposure-of-europes-ecosystems-to-ozone) accessed 23 June 2025.

Emberson, L. D., et al., 2000a, 'Modelling stomatal ozone flux across Europe', *Environmental Pollution* 109, pp. 403-413 (https://doi.org/10.1016/S0269-7491(00)00043-9) accessed 24 April 2025.

Emberson, L. D., et al., 2000b, *Towards a model of ozone deposition and stomatal uptake over Europe*, Norwegian Meteorological Institute, Research Note No. 42 (https://emep.int/publ/reports/2000/dnmi_note_6_2000.pdf) accessed 24 April 2025.

Emberson L.D., et al., 2018, 'Ozone effects on crops and consideration in crop models' *European Journal of Agronomy* 100, pp. 19-34 (https://doi.org/10.1016/j.eja.2018.06.002) accessed 24 April

ESA, 2019, *Land cover classification gridded maps from 1992 to present derived from satellite observations* (https://cds.climate.copernicus.eu/datasets/satellite-land-cover) accessed 4 May 2025.

EU, 2020, *Corine land cover 2018 (CLC2018) raster data*, 100 m gridded version 2020_20 (https://land.copernicus.eu/pan-european/corine-land-cover/clc2018) accessed 19 November 2020.

EU, 2024, *Directive (EU) 2024/2881 of the European Parliament and of the Council of 23 October 2024 on ambient air quality and cleaner air for Europe* (recast) (OJ L 2881, 20.11.2024) (https://eur-lex.europa.eu/eli/dir/2024/2881/oj) accessed 24 April 2025.

Fares, S., et al., 2010, 'Ozone fluxes in a Pinus ponderosa ecosystem are dominated by non-stomatal processes: Evidence from long-term continuous measurements', *Agricultural and Forest Meteorology* 150, pp. 420-431 (https://doi.org/10.1016/j.agrformet.2010.01.007) accessed 28 March 2022.

Fares, S., et al., 2013, 'Testing of models of stomatal ozone fluxes with field measurements in a mixed Mediterranean forest', *Atmospheric Environment* 67, pp. 242-251 (https://doi.org/10.1016/j.atmosenv.2012.11.007) accessed 26 May 2022.

Fares, S., et al., 2017, 'Ozone flux in plant ecosystems: new opportunities for long-term monitoring networks to deliver ozone-risk assessments', *Environmental Science and Pollution Research* 25, pp. 8240-8248 (https://doi.org/10.1007/s11356-017-0352-0) accessed 24 April 2025.

Fowler, W., et al., 2008, *Ground-Level Ozone in the 21st Century: Future Trends, Impacts and Policy Implications*, RS Policy document 15/08, The Royal Society, London (https://royalsociety.org/-/media/policy/publications/2008/7925.pdf) accessed 24 April 2025.

Fuhrer, J., 2002, 'Ozone impacts on vegetation', *Ozone: Science & Engineering* 24, pp. 69-74 (https://doi.org/10.1080/01919510208901597) accessed 24 April 2025.

González-Fernández, I., et al., 2013, 'Modelling ozone stomatal flux of wheat under Mediterranean conditions', *Atmospheric Environment* 67, pp. 149-160. (http://dx.doi.org/10.1016/j.atmosenv.2012.10.043) accessed 24 April 2025.

Grunhage L. et al., 2012, 'Updated stomatal flux and flux-effect models for wheat for quantifying effects of ozone on grain yield, grain mass and protein yield', *Environmental Pollution* 165, pp. 147-157 (https://doi.org/10.1016/j.envpol.2012.02.026) accessed 4 March 2026.

Haberle, J. and Svoboda, P., 2015, 'Calculation of available water supply in crop root zone and the water balance of crops', *Contributions to Geophysics and Geodesy* 45, pp. 285-298 (https://doi.org/10.1515/congeo-2015-0025) accessed 21 January 2021.

Heath, R. L., 2008, 'Modification of the biochemical pathways of plants induced by ozone: What are the varied routes to change?', *Environmental Pollution* 155, pp. 453-463 (https://doi.org/10.1016/j.envpol.2008.03.010) accessed 24 April 2025.

Horálek, J., et al., 2007, *Spatial mapping of air quality for European scale assessment*, ETC/ACC Technical paper 2006/6 (http://www.eionet.europa.eu/etcs/etc-atni/products/etc-atni-reports/etcacc_technpaper_2006_6_spat_aq) accessed 26 August 2020.

Horálek, J., et al., 2024, *Air quality maps of EEA member and cooperating countries for 2022*, Eionet Report ETC HE 2024/4 (https://doi.org/10.5281/zenodo.14639621*), updated version (forthcoming)*.

Horálek, J., et al., 2025, *Air quality maps of EEA member and cooperating countries for 2023*, Eionet Report ETC HE 2025/5 (https://doi.org/10.5281/zenodo.17427293) accessed 25 November 2025.

Jacob, D.J., et al., 1993, 'Factors regulating ozone over the United States and its export to the global atmosphere', *Journal of Geophysical Research* 98, pp. 14817–14826 (https://doi.org/10.1029/98JD01224) accessed 24 April 2025.

Jacob, D. J. and Winner, D. A., 2009, 'Effect of climate change on air quality'*, Atmospheric Environment* 43, pp. 51-63 (https://doi.org/10.1016/j.atmosenv.2008.09.051) accessed 24 April 2025.

Jarvis, P. G., 1976, 'The interpretation of the variation in leaf water potential and stomatal conductance found in canopies in the field', Philosophical Transactions of the Royal Society of London, Series B: *Biological Sciences* 273, pp. 593-610 (https://doi.org/10.1098/rstb.1976.0035) accessed 26 May 2021.

JRC, 2016, *Maps of indicators of soil hydraulic properties for Europe*, dataset/maps downloaded from the European Soil Data Centre (http://esdac.jrc.ec.europa.eu/content/maps-indicators-soil-hydraulic-properties-europe) accessed 8 December 2020.

Karlsson, P. E., et al., 2017, 'Past, present and future concentrations of ground-level ozone and potential impacts on ecosystems and human health in northern Europe', *Science of The Total Environment* 576, pp. 22-35 (https://doi.org/10.1016/j.scitotenv.2016.10.061) accessed 6 May 2022.

Matyssek, R., et al., 2007, 'Promoting the O_3 flux concept for European forest trees', *Environmental Pollution* 146, pp. 587-607 (https://doi.org/10.1016/j.envpol.2006.11.011) accessed 11 July 2022.

MDA, 2015, *World Land Cover at 30m resolution from MDAUS BaseVue 2013* (https://www.arcgis.com/home/item.html?id=1770449f11df418db482a14df4ac26eb) accessed 17 February 2021.

Mills, G., et al., 2011, 'New stomatal flux-based critical levels for ozone effects on vegetation', *Atmospheric Environment* 45, pp. 5064-5068 (https://doi.org/10.1016/j.atmosenv.2011.06.009) accessed 19 November 2020.

Mills, G., et al., 2018, 'Tropospheric Ozone Assessment Report: Present-day tropospheric ozone distribution and trends relevant to vegetation', *Elementa: Science of the Anthropocene* 6, pp. 47 (https://doi.org/10.1525/elementa.302) accessed 24 April 2025.

Mittler, R., 2002, 'Oxidative stress, antioxidants and stress tolerance', *Trends in Plant Science* 7, pp. 405-410 (https://doi.org/10.1016/S1360-1385(02)02312-9) accessed 27 April 2022.

Musselman, R. C. and Massman, W. J., 1998, 'Ozone flux to vegetation and its relationship to plant response and ambient air quality standards', *Atmospheric Environment* 33, pp. 65-73 (https://doi.org/10.1016/S1352-2310(98)00127-7) accessed 24 April 2025.

Musselman, R. C., et al., 2006, 'A critical review and analysis of the use of exposure- and flux-based ozone indices for predicting vegetation effects', *Atmospheric Environment* 40, pp. 1869-1888 (https://doi.org/10.1016/j.atmosenv.2005.10.064) accessed 11 July 2022.

NILU, 2024, *EBAS, database of atmospheric chemical composition and physical properties* (http://ebas-data.nilu.no). Data extracted in April 2024.

NILU, 2025, *EBAS, database of atmospheric chemical composition and physical properties* (http://ebas-data.nilu.no). Data extracted in March 2025.

Nolle, M., et al., 2002, 'A long-term study of background ozone concentrations in the central Mediterranean—diurnal and seasonal variations on the island of Gozo', *Atmospheric Environment* 36, pp. 1391-1402 (https://doi.org/10.1016/s1352-2310(01)00505-2) accessed 24 April 2025.

Nussbaum, S., et al., 2003, 'High-resolution spatial analysis of stomatal ozone uptake in arable crops and pastures', *Environmental International* 129, pp. 385-392 (https://www.ncbi.nlm.nih.gov/pubmed/12676231) accessed 26 May 2021.

Paoletti, E., 2006, 'Impact of ozone on Mediterranean forests: A review', *Environmental Pollution* 144, pp. 463-474 (https://doi.org/10.1016/j.envpol.2005.12.051) accessed 26 May 2022.

Pell, E. J., et al., 1997, 'Ozone induced oxidative stress: Mechanism of action and reaction', *Physiologia Plantarum* 100, pp. 264-273 (https://onlinelibrary.wiley.com/doi/pdf/10.1111/j.1399-3054.1997.tb04782.x) accessed 27 April 2022.

Pleijel, H., et al., 2007, 'Ozone risk assessment for agricultural crops in Europe: Further development of stomatal flux and flux-response relationships for European wheat and potato', *Atmospheric Environment* 41, pp. 3022-3040 (https://doi.org/10.1016/j.atmosenv.2006.12.002) accessed 8 December 2020.

Pedersen, S. M., et al., 2005, *Potato production in Europe - a gross margin analysis*, University of Copenhagen, FOI WorkingPaper Vol. 2005 No. 5, pp. 1-39 (https://curis.ku.dk/ws/files/135440168/5.pdf) accessed 26 May 2021.

Reich, P. B., 1987, 'Quantifying plant response to ozone: a unifying theory', *Tree Physiology* 3, pp. 63-91 (https://doi.org/10.1093/treephys/3.1.63) accessed 19 November 2020.

Reif, J., et al., 2023, 'Ambient ozone – New threat to birds in mountain ecosystems?', *Science of the Total Environment* 876, pp. 162711 (https://doi.org/10.1016/j.scitotenv.2023.162711) accessed 24 April 2025.

Ronan, A. C., et al., 2020, 'Have improvements in ozone air quality reduced ozone uptake into plants?', *Elementa: Science of the Anthropocene* 8(2) (https://doi.org/10.1525/elementa.399) accessed 26 May 2022.

Schraudner, M., et al., 1997, 'Changes in the biochemical status of plant cells induced by the environmental pollutant ozone', *Physiologia Plantarum* 100, pp. 274-280 (https://doi.org/10.1111/j.1399-3054.1997.tb04783.x) accessed 26 May 2022.

Schucht, S., et al., 2024, *Wheat and potato yield loss in 2022 in Europe due to ozone exposure,* ETC HE Report 2024/9 (https://doi.org/10.5281/zenodo.14699280) accessed 7 January 2026.

Simpson, D., et al., 2012, 'The EMEP MSC-W chemical transport model – technical description', *Atmospheric Chemistry and Physics* 12, pp. 7825-7865 (https://doi.org/10.5194/acp-12-7825-2012) accessed 26 August 2020.

Annex 1 Methodology

A1.1 Phytotoxic Ozone Dose above a threshold flux Y (POD_Y) calculation

The calculation of the phytotoxic O_3 dose, as outlined below, follows the methodology described in the Manual for modelling and mapping critical loads & levels of the Long-Range Transboundary Air Pollution Convention (CLRTAP) in its most recent available revision (CLRTAP, 2024), including some specifications presented in the Scientific background documents of this manual (CLRTAP, 2017, 2020), as prepared by the International scientific Cooperative Programme on effects of air pollution on natural vegetation and crops of the Working Group on Effects of the CLRTAP (ICP Vegetation). The steps to be taken are presented in Table A1.1.

Table A1.1 Steps to be taken to calculate exceedance of flux-based (POD_YSPEC or POD_YIAM) critical levels

1	Decide on the species and biogeographical region(s) to be included.
2	Obtain the O_3 concentrations at the top of the canopy for the species or vegetation-specific accumulation period.
3	Calculate the hourly stomatal conductance of O_3 (g_{sto}).
4	Model the hourly stomatal flux of O_3 (F_{sto}).
5	Calculation of POD_Y (POD_YSPEC or POD_YIAM) from F_{sto}.

Source: CLRTAP, 2024.

The cumulative stomatal O_3 fluxes (F_{sto}) are calculated over the course of the growing season based on ambient O_3 concentration and stomatal conductance (g_{sto}) to O_3. g_{sto} is calculated using a multiplicative stomatal conductance model proposed by Jarvis (1976) and modified by Emberson et al. (2000a) as a function of species-specific maximum g_{sto} (expressed on a projected leaf-area basis), phenology, and prevailing environmental conditions (photosynthetic photon flux density (PPFD)), air temperature, vapour pressure deficit (VPD), and soil moisture.

Hourly averaged stomatal O_3 fluxes (F_{sto}) in excess of a threshold Y (expressed in mmol/m^2 PLA ([1])) are accumulated over a species or vegetation-specific accumulation period during daylight hours, in order to get the phytotoxic O_3 dose above the threshold Y (POD_Y).

Two POD_Y versions are available in CLRTAP (2017a): POD_YIAM (which is a simplified version recommended for Integrated Assessment Modelling) and POD_YSPEC (which is specific to a given specie). Here, the calculation of POD_YSPEC for wheat and potato (labelled further simply as POD_6 for wheat and potato) is presented. Simplifications and differences in the calculation of POD_3IAM for crops compared to POD_6SPEC for wheat and potato are provided in Box 2.

([1]) PLA, or the projected leaf area, is the total area of the sides of the leaves that are projected towards the sun. PLA is different to the total leaf area, which accounts for both sides of the leaves.

Box 2 Simplifications and differences in the calculation of POD_YIAM compared to POD_YSPEC

A flux-threshold Y

Due to difficulties in estimating the O_3 flux using Y = 6 nmol/m^2 PLA per second in large scale modelling and IAM arising from the strong increase in the uncertainty in modelled POD with increasing Y, Y= 3 nmol/m^2 PLA per second is to be used (POD_3IAM).

f_{phen} and f_{O3}

The simplified flux models suitable for POD_YIAM do not include the modifying effect of phenology and O_3 in the case of crops on the stomatal conductance, hence f_{phen} and f_{O3} for crops are set to 1 between the start and the end of the accumulation period.

f_{SW}

The simplified flux models suitable for IAM do not include the modifying effect of soil moisture on the stomatal conductance, hence f_{SW} is set to 1 between the start and the end of the accumulation period. Using the simplified flux models as a stand-alone application, this method would indicate the risk of O_3 damage under the worst case scenario where soil moisture is not limiting stomatal O_3 flux. However, the effect of soil moisture is important and in large-scale applications, surrogate indices are usually applied such as the Soil Moisture Index in the EMEP model (Simpson et al., 2012). Thus, f_{SMI} (where *SMI* represents the Soil Moisture Index) as routinely used in the calculations of POD_6SPEC for wheat and potato is used in this report also for the calculation of POD_3IAM for crops.

A_{start}_ETS and A_{end}_ETS

To accommodate the need for IAM to use a longer time period than the thermal time-based time window used for POD_6SPEC, POD_3IAM is accumulated over 90 days, centred on the timing of mid-anthesis (flowering) in wheat. Therefore, A_{start}_ETS and A_{end}_ETS are set to be 45 days before mid-anthesis in wheat and 45 days after mid-anthesis in wheat, respectively.

Source: CLRTAP, 2024

Obtaining the ozone concentrations at the top of the canopy for the species or vegetation-specific accumulation period

The O_3 concentration at the top of the canopy (nmol/m^3) in the given hour H is calculated according to

$$c(z_1) = c(z_{m,O3}) * \left[1 - \frac{R_a(z_{tgt},\ z_{m,O3})}{R_a\left(d+z_0,\ z_{m,O3}\right) + R_b + R_{surf}}\right] \quad \text{(A1.1)}$$

where
- $c(z_1)$ is O_3 concentration at the top of the canopy,
- $c(z_{m,O3})$ is the O_3 concentration estimated based on measurements at the height z_m, (see Eq. A1.6),
- $R_a(x, y)$ is the aerodynamic resistance between the height of y and the height of x,
- R_b is the resistance to O_3 diffusion in the laminar sub-layer,
- R_{surf} is the overall resistance to O_3 deposition to the underlying surfaces,

while

$$R_a(z_{tgt},\ z_{m,O3}) = \frac{1}{k.u*}\left[ln\left(\frac{z_{m,O3}-d}{z_{tgt}-d}\right) - \Psi_H\left(\frac{z_{m,O3}-d}{L}\right) + \Psi_H\left(\frac{z_{tgt}-d}{L}\right)\right] \quad \text{(A1.1a)}$$

$$R_a(d+z_0,\ z_{m,O3}) = \frac{1}{k.u*}\left[ln\left(\frac{z_{m,O3}-d}{z_0}\right) - \Psi_H\left(\frac{z_{m,O3}-d}{L}\right) + \Psi_H\left(\frac{z_0}{L}\right)\right] \quad \text{(A1.1b)}$$

$$R_b = \frac{2}{k\ .u*}\left(\frac{Sc}{Pr}\right)^{2/3} \quad \text{(A1.1c)}$$

$$R_{surf} = \frac{1}{\frac{LAI}{R_{sto}} + \frac{SAI}{R_{ext}} + \frac{1}{R_{inc}+R_{soil}}} \quad \text{(A1.1d)}$$

where
- k is the von Kármán constant (equal to 0.41),
- z_{tgt} is the top canopy height (the target height),
- $z_{m,O3}$ is the height of the available O_3 measurement above the canopy,

z_0 is the roughness length, usually assumed as 1/10 of the canopy height,
L is the Obukhov length,
d is the displacement height, usually assumed as 2/3 of the canopy height,
u^* is the friction velocity,
Sc is the Schmidt number for O_3 (equal to 0.41),
Pr is the Prandtl number of air (equal to 0.71),
LAI is the projected leaf area in (m^2/m^2),
SAI is the surface area of the canopy in (m^2/m^2),
$\Psi_H(..) = \Psi_H(\zeta)$ is the similarity function for heat with ζ as the argument ([2]),

according to

$$(\zeta) = 2 \quad \text{when } \zeta < 0$$
$$= -5\zeta \quad \text{when } \zeta \geq 0 \qquad \text{(A1.1e)}$$

with $x = (1 - 16 * \zeta)^{1/4}$ (A1.1f)

and R_{ext} is the resistance to cuticular deposition of O_3 (equal to 2,500 s/m);
R_{soil} is the soil resistance (equal to 200 s/m^1),
while $R_{sto} = 1/g_{sto}$ (A1.1g)
$R_{inc} = b.SAI.h/u^*$ (A1.1h)

where g_{sto} is the actual stomatal conductance,
b is the empirical constant (equal to 14 m^{-1}),
h is the height of the canopy.

The calculations of LAI and SAI are based on Simpson et al. (2012) and Emberson et al. (2000b), as well as the schematics regarding LAI presented therein (see Eq. 2.8i to 2.8n).

$LAI = LAI_{min} + (d - SGS) * (LAI_{max} - LAI_{min}) / SGS_{length}$, (A1.1i)
$SAI = 5 * LAI / 3.5$ (A1.1j)
when $SGS \leq d < SGS + SGS_{length}$
$LAI = LAI_{max}$, (A1.1k)
$SAI = LAI + 1.5$, (A1.1l)
when $SGS + SGS_{length} \leq d < EGS - EGS_{length}$
$LAI = LAI_{max} - (d - (EGS - EGSlength)) * (LAI_{max} - LAI_{min}) / EGS_{length}$, (A1.1m)
$SAI = LAI + 1.5$, (A1.1n)
when $EGS - EGSlength \leq d < EGS$

where LAI_{min} is the minimum (within the growing season) LAI values (m^2/m^2)
LAI_{max} is the maximum (within the growing season) LAI values (m^2/m^2)
SGS is the start of the growing season (day of year)
SGS_{length} is the duration of the start of the growing season (days)
EGS_{length} is the duration of the end of the growing season (days)
EGS is the end of the growing season (day of year)

Calculation of the hourly stomatal conductance of ozone (g_{sto})

The basis of the approach used for calculating phytotoxic O_3 doses is the calculation of an instantaneous stomatal conductance g_{sto} in the given hour H, according to the equation

([2]) For more details see CLRTAP (2017).

$$g_{sto} = g_{max} * [min(f_{phen}, f_{O3})] * f_{light} * max[f_{min}, (f_{temp} * f_{VPD} * f_{SW})] \quad \text{(A1.2)}$$

where
- g_{sto} is the actual stomatal conductance in (mmol O_3 /m^2 PLA per second),
- g_{max} is the species-specific maximum stomatal conductance in (mmol O_3 /m^2 PLA per second), see Table A1.3,
- f_{phen} is the relative proportion function for the phenology for the different stage of growing; for POD_YIAM, f_{phen} is set to 1 (see Box 2),
- f_{O3} is the relative proportion function for the influence of O_3 on stomatal flux by promoting premature senescence; for POD_YIAM, f_{phen} is set to 1 (see Box 2),
- f_{min} is the species-specific relative minimum stomatal conductance that occurs during daylight hours, see Tables A1.3 and A1.4,
- f_{temp}, f_{VPD}, f_{SW}, f_{light} are relative proportion functions for leaf stomata respond to temperature, air humidity, soil moisture and light.

Parameters f_{phen}, f_{O3}, f_{light}, f_{temp}, f_{VPD}, f_{SW} and f_{min} are expressed as relative proportion functions, taking values between 0 and 1 as a proportion of g_{max}. These functions allow taking into account irradiance (f_{light}), temperature (f_{temp}), water vapour deficit at leaves level (f_{VPD}), soil moisture (f_{sw}), phenology for the different stage of growing (f_{phen}) and the influence of O_3 on stomatal flux by promoting premature senescence (f_{O3}). f_{min} is the minimum relative value of stomatal conductance during the daylight.

The parameter f_{phen} is calculated based on the accumulation of thermal time over the growing season of the crop being considered (Colette et al., 2018), according to CLRTAP (2024)). For wheat and potato, the accumulation period is defined for each year using the effective temperature sum (*ETS*) in ˚C for days in excess of 0 ˚C.

For wheat, the total accumulation period during which wheat is sensitive to O_3 exposure is 200 °C days and 300 °C days before mid-anthesis (mid-point in flowering) to 700 °C days to 550 °C days after mid-anthesis for Atlantic, Boreal and Continental regions and Mediterranean region, respectively. The timing of mid-anthesis is estimated by starting at the first date after 1 January (or just 1 January) when the temperature exceeds 0 °C. The mean daily temperature is then accumulated (temperature sum), and mid-anthesis is estimated to be a temperature sum of 1,075 °C days for Atlantic, Boreal and Continental regions and 1,250 °C days for Mediterranean region, which in general corresponds to bread wheat.

For potato, the accumulation period stands between 330 °C days before the tuber initiation date and 800 °C days after this date. The tuber initiation date is considered to be homogeneous throughout Europe. The reasons for its simplification are a) heterogeneous climatic conditions in the European countries naturally lead to different time of potato planting (Pedersen et al., 2005) followed by different time of the tuber initiation and b) lack of detailed local data availability for. As discussed ([3]) with the French national Chamber of agriculture (APCA, http://chambres-agriculture.fr), the tuber initiation starts 15 days after the transplantation in the field, which occurs in May. Therefore, the fixed date for the tuber initiation was set to June 1st.

The accumulation period for POD_3IAM is defined as a 90-day time window centred on the timing of mid-anthesis (flowering) in wheat. Consequently, the start of the accumulation period (A_{start}) is set to

([3]) There is a lack of information on a date of potato tuber initiation in Europe. It should ideally rely on existing models based on agricultural practices, local climatology, ground properties, and location. INERIS, while developing the POD script, relied on contents of discussions with the French National Chamber of Agriculture (consultation with APCA, March 2018; Deumier and Hannon, 2010). Based on the information given that the tuber initiation starts 15 days after the transplantation in the field, which occurs in May in France, a fixed date of June 1st has been chosen for France and applied also for the rest of Europe. This date should be revised according to the availability of more accurate information on potato plantations in Europe.

45 days before mid-anthesis, and the end of the accumulation period (A_{end}) is set to 45 days after mid-anthesis; see Table A1.4.

The parameter f_{phen} is calculated according to following equations:

in the case of wheat:

$$f_{phen} = 1 \quad \text{when} \quad (f_{phen\_2\_ETS} + f_{phen\_1\_ETS}) \leq ETS \leq (f_{phen\_2\_ETS} + f_{phen\_3\_ETS})$$

$$f_{phen} = 1 - \left(\frac{f_{phen\_a}}{f_{phen\_4\_ETS} - f_{phen\_3\_ETS}}\right) * (ETS - f_{phen\_3\_ETS}) \quad \text{when} \quad (f_{phen\_2\_ETS} + f_{phen\_3\_ETS}) < ETS \leq (f_{phen\_2\_ETS} + f_{phen\_4\_ETS})$$

$$f_{phen} = f_{phen\_e} - \left(\frac{f_{phen\_e}}{f_{phen\_5\_ETS} - f_{phen\_4\_ETS}}\right) * (ETS - f_{phen\_4\_ETS}) \quad \text{when} \quad (f_{phen\_2\_ETS} + f_{phen\_4\_ETS}) < ETS \leq f_{phen\_5\_ETS} \qquad \text{(A1.2a)}$$

in the case of potato (formulated based on CLRTAP, 2017):

$$f_{phen} = 1 - \left(\frac{1 - f_{phen\_a}}{f_{phen\_1\_ETS}}\right) * ETS \quad \text{when} \quad f_{phen\_1\_ETS} \leq ETS < 0$$

$$f_{phen} = 1 - \left(\frac{1 - f_{phen\_e}}{f_{phen\_2\_ETS}}\right) * ETS \quad \text{when} \quad 0 < ETS \leq f_{phen\_2\_ETS} \qquad \text{(A1.2b)}$$

in the case of POD$_3$IAM :

$$f_{phen} = 1 \qquad \text{(A1.2c)}$$

where *ETS* is the effective temperature sum in ˚C days using a base temperature of 0 ˚C for wheat and potato (see Table A1.3);
for wheat, ETS is set to 0 °C days at mid-anthesis day. Then A_{start_ETS} will be at 200 ˚C days before mid-anthesis, and A_{end_ETS} will be at 700 ˚C days after mid-anthesis over a base temperature of 0 °C;
for potato, ETS is set to 0 °C days at tuber initiation day. Then A_{start_ETS} will be at 330 ˚C days before tuber initiation and A_{end_ETS} at 800 ˚C days after tuber initiation over a base temperature of 0 °C;

f_{phen_a}, f_{phen_e} is the phenology function, which consists of terms describing rate changes of g_{max} expressed as fractions (see Table A1.3),

$f_{phen\_1\_ETS}$, $f_{phen\_2\_ETS}$, $f_{phen\_3\_ETS}$, $f_{phen\_4\_ETS}$, $f_{phen\_5\_ETS}$ are °C days (see Table A1.2; $f_{phen\_1\_ETS}$ and $f_{phen\_5\_ETS}$ define period crops to be sensitive to O_3 exposure),

A_{start_ETS} and A_{end_ETS} are the start and the end of the accumulation period based on the effective temperature sums (counted from the day of the mid-anthesis for wheat and from the day of the tuber initiation for potato) above a base temperature of 0 ˚C for both wheat and potato at the start and end of the O_3 accumulation period; for POD$_3$IAM, see Table A1.4.

The parameter f_{O3} in the case of wheat is calculated according to equation

$$f_{O3} = [(1+(POD_0/14)^8]^{-1} \qquad \text{(A1.2d)}$$

while $$POD_0 = \sum_{n=A_{start}}^{H-1} F_{sto}(n) \cdot \frac{3600}{10^6} \qquad \text{(A1.2e)}$$

where POD_0 is the O_3 flux already accumulated since the beginning of the vegetation period A_{start} up to the last hour *H-1*,

$F_{sto}(n)$ is the hourly O_3 flux in the hour n, calculated in the previous steps based on Equation 2.10, while $F_{sto}(A_{start})$ is equal to 0.

In the case of potato, the parameter (O_3 function) f_{O3} is calculated according to equation

$$f_{O3} = [(1+(AOT0/40)^5]^{-1} \quad \text{(A1.2f)}$$

where *AOT0* is accumulated O_3 concentration from the start of the vegetation period A_{start} up to the last hour *H-1*.

In the case of POD_3IAM, the parameter f_{O3} is set to 1.

The parameter f_{light} is calculated according to

$$f_{light} = 1 - EXP[(-light\_a)*PPFD] \quad \text{(A1.2g)}$$

while $$PPFD = SSRD * 0.5 * 4.5 \quad \text{(A1.2h)}$$

where *PPFD* represents the photosynthetic photon flux density (µmol/m^2 per second),
light_a is a light parameter (see Tables A1.3 and A1.4),
SSRD represents the surface net solar radiation in (W/m^2).

The parameter f_{temp} is calculated according to:

$$f_{temp} = \max \{f_{min}, [(T - T_{min}) / (T_{opt} - T_{min})] * [(T_{max} - T) / (T_{max} - T_{opt})]^{bt}\} \quad \text{when } T_{min} < T < T_{max}$$
$$= f_{min} \quad \textit{when } T_{min} > T > T_{max} \quad \text{(A1.2i)}$$

while $$bt = (T_{max} - T_{opt}) / (T_{opt} - T_{min}) \quad \text{(A1.2j)}$$

where T_{min}, T_{max} and T_{opt} are minimum, maximum and optimum temperatures determining leaf stomata opening (see Tables A1.3 and A1.4)

The parameter f_{VPD} is calculated according to:

$$f_{VPD} = \min\{1,\max \{f_{min}, [(1-f_{min})*(VPD_{min} - VPD) / (VPD_{min} - VPD_{max})] + f_{min}\}\} \quad \text{(A1.2k)}$$

while $$VPD = e_s(Ta) * (1-hr) \quad \text{(A1.2l)}$$
$$e_s(Ta) = a \exp[bT_a/(T_a+c)] \quad \text{(A1.2m)}$$

where VPD_{min} is the minimum vapour pressure deficit determining leaf stomata opening (see Tables A1.3 and A1.4),
VPD_{max} is the maximum vapour pressure deficit determining leaf stomata opening (see Tables A1.3 and A1.4),
T_a is the air temperature (°C),
h_r is the relative humidity (%)/100,
$e_s(Ta)$ is the potential (saturation) water vapour pressure,
a, *b*, *c* are the empirical constants (a = 0.611 kPa, b = 17.502, c = 240.97 °C).

The ΣVPD (i.e. the function describing stomatal re-opening in the afternoon) is taken into account for maps POD_YSPEC for wheat and potato. ΣVPD (kPa) should be calculated for daylight hours until dawn of the next day. If ΣVPD ≥ ΣVPD_crit, g_{sto} calculated using Equation A1.2 is valid if smaller or equal to g_{sto} of the preceding hour. If g_{sto} is larger than g_{sto} of the preceding hour, given that ΣVPD is larger than or equal to ΣVPD_crit, it is replaced by the g_{sto} of the preceding hour.

The parameter f_{SW} is replaced by f_{SMI} (where *SMI* represents Soil Moisture Index with maximum at field capacity), taking values between 0 and 1 as a proportion of g_{max} (with 0 for soil moisture at and below

wilting point), following the parameterization given in Simpson et al. (2012), similar to the plant available water (*PAW*) parameterization f_{PAW} as defined for wheat in CLRTAP (2017a). The basic equation used for f_{SW} resp. f_{SMI} is:

$$\begin{aligned} f_{SMI} &= 0 && \text{for SMI} \le 0 \\ &= \frac{\text{SMI}}{\text{PAW}_t} && \text{for } 0 < \text{SMI} \le PAW_t \\ &= 1 && \text{for SMI} > PAW_t \end{aligned} \qquad \text{(A1.2n)}$$

while $$\text{SMI} = \frac{\text{SWLL} - \text{PWP}}{\text{FC} - \text{PWP}} \qquad \text{(A1.2o)}$$

where
- PAW_t is the threshold amount of water in the soil available to the plants, above which stomatal conductance is at a maximum, set to 0.5 (see Tables A1.3 and A1.4),
- *SWLL* is the soil moisture in (m^3/m^3),
- *PWP* is the permanent wilting point in (cm^3/cm^3),
- *FC* is the field capacity in (cm^3/cm^3).

The Soil Moisture Index using the EMEP methodology as described in Simpson et al. (2012) and CLRTAP (2020) is used. It is computed using the soil moisture variable available from a meteorological model, which represents the water content in m^3 of water per m^3 of ground (m^3/m^3) in a specific ground level, in dependence on the available dataset. For soil moisture, the ECWMF's ERA5-Land variable Volume of water in soil layer 3 (i.e. 28-100 cm) has been used, see Annex 2, Section A2.1. The level of soil layer was chosen based on recommendation of Haberle and Svoboda (2015). The soil moisture is quite a sensitive parameter in the calculation of the POD. Next to the soil moisture, the soil moisture index also takes into account the permanent wilting point and the field capacity; they are taken from JRC soil database (JRC, 2016), see Annex 2, Section A2.1.

Modelling the hourly stomatal flux of ozone (F_{sto})

Once the hourly stomatal conductance of O_3 (g_{sto}) and all relevant variables are computed, the stomatal flux of O_3 (F_{sto}) can be calculated, based on the assumption that the concentration of O_3 at the top of the canopy represents a reasonable estimate of the concentration at the upper surface of the laminar layer for a sunlit upper canopy leaf. F_{sto} is calculated according to the CLRTAP (ICP Vegetation) methodology, thus the fraction of the O_3 taken up by the stomata is given using a combination of the stomatal conductance, the quasi-laminar resistance and the leaf surface resistance (which depends on the external leaf, or cuticular, resistance). The hourly stomatal flux in the given hour H is calculated according to

$$F_{sto} = c(z_1) * g_{sto} * \frac{r_c}{r_b + r_c} \qquad \text{(A1.3)}$$

where
- F_{sto} is the hourly stomatal flux of O_3 in (nmol/m^2 PLA per second)
- $c(z_1)$ is the concentration of O_3 at canopy top in (nmol/m^3)
- r_b is the quasi-laminar resistance in (s/m)
- r_c is the leaf surface resistance in (s/m)
- g_{sto} is the actual stomatal conductance in (m/s),

while $r_c = 1/(g_{sto} + g_{ext})$ (A1.3a)

$$r_b = 1.3 * 150 * \sqrt{\frac{L}{u(z_1)}} \qquad \text{(A1.3b)}$$

where
- g_{ext} is the external leaf, or cuticular, resistance in (m/s), equal to 1/2,500 m/s
- $u(z_1)$ is the wind speed at height z_1 (z_1 is the canopy top)
- *L* is the cross-wind leaf dimension (2 cm or 4 cm, see Tables A1.3 and A1.4)

while $u_{(z1)} = \frac{u*}{k} * ln\,(\frac{z_1 - d}{z_0})$ for wheat

$= \frac{u*}{k} * ln\,(\frac{z_1}{z_0})$ for potato (A1.3c)

where
- k is the von Kármán constant (equal to 0.41)
- d is the displacement height usually assumed as 2/3 of the canopy height,
- z_1 is the top of the canopy
- z_0 is the roughness length usually assumed as 1/10 of the canopy height
- $u*$ is the friction velocity.

Box 3 Conversion of stomatal conductance g_{sto} and ozone concentration to units demanded for POD_Y calculation

Stomatal conductance g_{sto} has to be converted from units mmol/m^2 per second to units m/s (since all the resistances are expressed in the unit of s/m). At standard temperature (20 °C) and air pressure (1.013 x 10^5 Pa), the conversion is made by dividing the conductance in mmol/m^2 per second by 41,000 to give conductance in m/s.

To convert the **O_3 concentration (C)** at canopy height from µg/m^3 resp. ppb to nmol/m, the following equation should be used:

$$C\ (\text{nmol}\cdot\text{m}^{-3}) = C\ (\text{ppb}) * P/(R\cdot T) = C\ (\mu\text{g/m}^3) / 2 * P/(R\cdot T) \quad \text{(A1.4)}$$

where
- P is the atmospheric pressure in Pa,
- R is the universal gas constant of 8.31447 J/mol per Kelvin
- T is the air temperature in Kelvin.

At standard temperature (20 °C) and air pressure (1.013 x 10^5 Pa), the concentration in ppb should be multiplied by 41.56 to calculate the concentration in nmol/m^3.

Source: CLRTAP, 2024

Calculation of POD_Y from F_{sto}

Hourly averaged stomatal O_3 fluxes (F_{sto}) in excess of a Y threshold are accumulated over a species or vegetation-specific accumulation period using the following equation:

$$POD_Y = \sum_n (F_{sto}(n) - Y) \cdot \frac{3600}{10^6} \quad \text{(A1.5)}$$

while Y = 6 nmol/m^2 PLA per second (for POD_YSPEC for wheat or potato)

Y = 3 nmol/m^2 PLA per second (for POD_YIAM)

where
- POD_Y is the phytotoxic ozone dose related to the threshold Y, in (mmol/m^2 PLA),
- $F_{sto}(n)$ is the hourly ozone flux in the hour n of the accumulation period.

The value Y (in (nmol/m^2 PLA per second)) is subtracted from each hourly averaged F_{sto} (in (nmol/m^2 PLA per second)) value and the F_{sto} (after the subtracting of Y) is accumulated only when F_{sto}>Y, during daylight hours (when global radiation is more than 50 W/m^2). The value is then converted to hourly fluxes by multiplying by 3,600 and to mmol by dividing by 10^6 to get the stomatal ozone flux in mmol/m^2 PLA.

Critical levels of POD_Y

Table A1.2 shows critical levels (CLs) for crops as set by CLRTAP.

Table A1.2 POD_6SPEC and POD_3IAM critical levels (CL) for crops

Species	Effect parameter	Critical Levels (CL)	
		POD_6SPEC	POD_3IAM
Wheat	Grain yield	1.3	-
Wheat	1,000-grain weight	1.5	-
Wheat	Protein yield	2.0	-
Potato	Tuber yield	3.8	-
Crops	Grain yield	-	7.9

Source: CLRTAP, 2024.

A1.2 POD_Y parametrisation

Table A1.3 Parametrisation for POD_6SPEC for wheat flag leaves and the upper-canopy sunlit leaves of potato, for different biogeographical regions

Parameter	Units	(Bread) Wheat		Potato
		Atlantic, Boreal, Continental *(Pannonia, Steppic)*	Mediterranean	Atlantic, Boreal, Continental *(Mediterranean Pannonia, Steppic)*
g_{max}	mmol O_3 /m^2 PLA per second	500	430	750
f_{min}	fraction	0.01	0.01	0.01
light_a	-	0.0105	0.0105	0.005
T_{min}	°C	12	12	13
T_{opt}	°C	26	28	28
T_{max}	°C	40	39	39
VPD_{max}	kPa	1.2	3.2	2.1
VPD_{min}	kPa	3.2	4.6	3.5
ΣVPD_crit	kPa	8	16	10
PAW_t		0.5	0.5	0.5
f_{O3}	POD mmol O_3/m^2 PLA per second	14	-	-
f_{O3}	AOT0, ppmh	-	-	40
f_{O3}	exponent	8	-	5
SGS	ºC day	A_{start}_ETS	A_{start}_ETS	A_{start}_ETS
EGS	ºC day	A_{end}_ETS	A_{end}_ETS	A_{end}_ETS
SGS_{length}	days	70	70	35
EGS_{length}	days	22	44	65
LAI_{min}	m^2/m^2	0	0	0
LAI_{max}	m^2/m^2	5	3.5	6
Leaf dimension	cm	2	2	4
Canopy height	m	1	0.75	1
f_{phen_a}	fraction	0.3	0.5	0.4
f_{phen_e}	fraction	0.7	0.5	0.2
$f_{phen\_1\_ETS}$	°C day	-200	-300	-330
$f_{phen\_2\_ETS}$	°C day	0	0	800
$f_{phen\_3\_ETS}$	°C day	100	70	-
$f_{phen\_4\_ETS}$	°C day	525	312	-
$f_{phen\_5\_ETS}$	°C day	700	550	-
mid-anthesis	°C day	1,075	1,250	-

Source: CLRTAP, 2024; González-Fernández et al., 2013; González-Fernández (personal communication, May 2021); Emberson et al., 2000b; Simpson et al., 2012.

Table A1.4 Parametrisation for POD_3IAM for flag leaves for crops, based on (bread) wheat

Parameter	Units	Atlantic, Boreal, Continental, Pannonia, Steppic	Mediterranean
g_{max}	mmol O_3 /m^2 PLA per second	500	430
f_{min}	fraction	0.01	0.01
light_a	-	0.0105	0.0105
T_{min}	°C	12	13
T_{opt}	°C	26	28
T_{max}	°C	40	39
VPD_{max}	kPa	1.2	3.2
VPD_{min}	kPa	3.2	4.6
ΣVPD_crit	kPa	8	8
PAW_t		0.5	0.5
f_{O3}	POD_0 mmol O_3/m^2 PLA per second	1	1
A_{start}_ETS	ºC day	45 days before mid-anthesis*	45 days before mid-anthesis*
A_{end}_ETS	ºC day	45 days after mid-anthesis*	45 days after mid-anthesis*
SGS	ºC day	A_{start}_ETS	A_{start}_ETS
EGS	ºC day	A_{end}_ETS	A_{end}_ETS
SGS_{length}	days	70	70
EGS_{length}	days	22	44
LAI_{min}	m^2/m^2	0	0
LAI_{max}	m^2/m^2	5	3.5
Leaf dimension	cm	2	2
Canopy height	m	1	1
f_{phen}		1	1
mid-anthesis	°C day	1,075	1,250

Notes: * 90d accumulation period, centred on the timing of mid-anthesis in wheat, see Section A1.1, Box 2 for details.

Source: CLRTAP, 2024; González-Fernández et al., 2013; González-Fernández (personal communication, May 2021); Emberson et al., 2000b; Simpson et al., 2012.

Map A1.1 Biogeographical regions in Europe

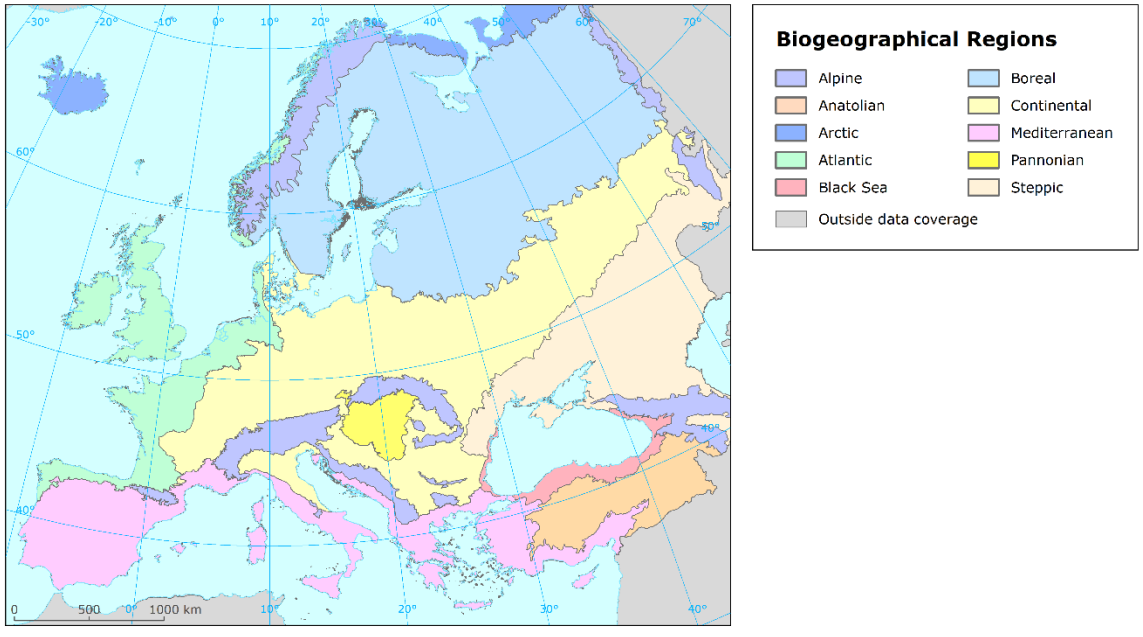

Source: EEA, 2016.

A1.3 Calculation of POD_Y spatial maps

Calculation of ozone spatial maps

The mapping method used is a linear regression model (using O_3 monitoring data from rural stations as a dependent variable and the chemical transport model results, altitude and solar radiation data as regressors) followed by kriging of the residuals produced from that model, according to the relation:

$$\hat{Z}(s_0) = c + a_1 \mathrm{M}(s_0) + a_2 A(s_0) + a_3 \mathrm{SSR}(s_0) + \hat{R}(s_i) \qquad \text{(A1.6)}$$

where $\hat{Z}(s_0)$ is the estimated O_3 value at the point s_o,

$M(s_0)$, $A(s_0)$, $SSR(s_0)$ are the chemical transport modelling (CTM), altitude and surface solar radiation values at the point s_o,

c, a_1, a_2, a_3 are the parameters of the linear regression model calculated based on the O_3 monitoring and the supplementary data at the measurement points,

$\hat{R}(s_i)$ is the spatial interpolation of the residuals of the linear regression model at the point s_o calculated based on the residuals at the measurement points.

Ordinary kriging is used to interpolate the residuals:

$$\hat{R}(s_i) = \sum_{i=1}^{N} \lambda_i R(s_i) \,, \sum_{i=1}^{N} \lambda_i = 1 \qquad \text{(A1.6a)}$$

where $R(s_i)$ are the residuals in the points of the measuring stations s_i,

$\lambda_1, \ldots, \lambda_N$ are the weights estimated based on the variogram,

N is the number of the stations used in the interpolation.

The variogram (as a measure of a spatial correlation) is estimated using a spherical function (with parameters nugget, sill, range). For details, see Horálek et al. (2007), Section 2.3.5 and Cressie (1993).

Calculation of POD_Y maps

During the POD_Y maps calculation, different biogeographical regions are considered. Plant stomatal functioning varies per plant species and can vary by biogeographical region, reflecting different adaptations of plants to climate and soil water in these regions. Parametrization for POD_6 (i.e. for wheat and potato) is currently available for all different biogeographic regions of Europe apart from Alpine region, i.e. for Atlantic, Boreal, Continental, Pannonian, Steppic, and Mediterranean regions (CLRTAP, 2017a). In the case of wheat, the parametrization is the same for most of these regions (namely Atlantic, Boreal, Continental, Pannonian, and Steppic), while for Mediterranean regions is different. For Alpine region, the parametrisation of the Continental and several other regions are used. For potato, only one parametrisation exists – it is set for all regions apart from the Alpine one. In the calculations, the existing parametrisation has been applied for the entire mapping area.

The values calculated in 0.1° x 0.1° resolution were converted into the standard ETRS89-LAEA5210 projection and transferred into the EEA 2 km resolution grid.

A1.4 Calculation of vegetation exposure

Vegetation exposure for individual countries, large European regions, EU-27, EEA-32, EEA-38, and for the total mapping area is calculated based on the POD_Y maps in the 2 km resolution and either the land cover data in the 100 m resolution or agricultural data in 1 km resolution. For each POD_Y class, the total agricultural area per country and large region, as well as European-wide is determined.

In addition, the exposure for individual countries, large regions, EU-27, EEA-32, EEA-38 and the whole area is expressed also as the agricultural area weighted concentration, i.e. the average POD_Y value across the relevant agricultural area.

For the designation of the large regions, see Map A1.2. For details, see Horálek et al. (2024). Although the biogeographical regions (see Map A1.1) are more relevant in the context of POD_Y, the large European regions are used for consistency with the exposure estimates of other indicators, including AOT40.

Map A1.2 Five large European regions

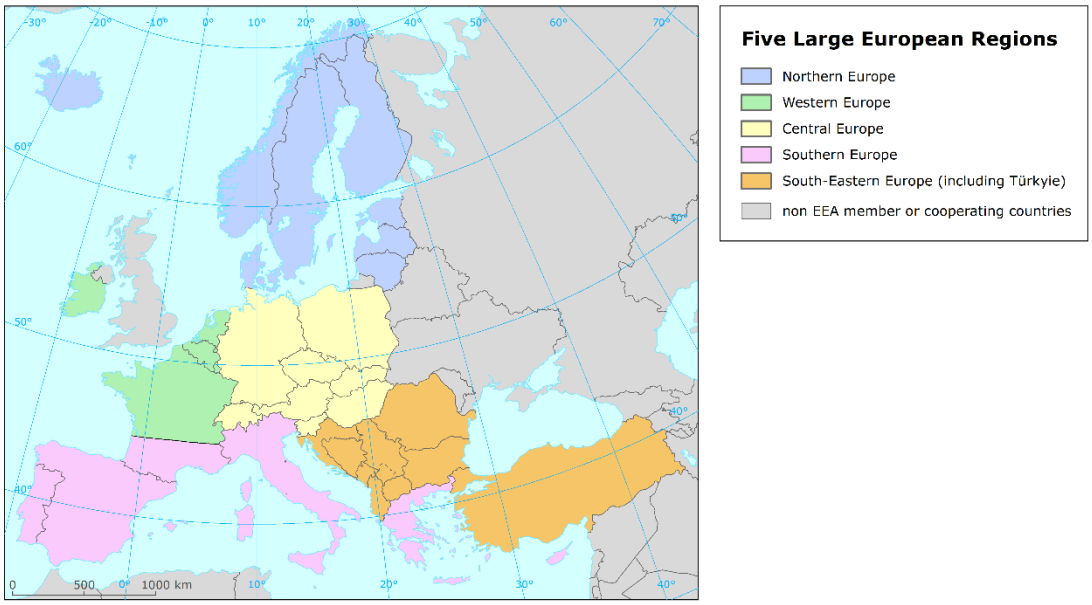

Annex 2 Input data

A2.1 Data needed for calculation of POD_Y maps

Air quality monitoring data

Air quality station monitoring data for the relevant year as extracted from the official EEA Air Quality e-Reporting database, EEA (2024, 2025a) in March 2024 and February 2025 have been used. This data set has been supplemented with British stations from the Defra (2024, 2025) database ([4]) and with several EMEP rural stations from the EBAS (NILU, 2024, 2025) database not reported to the Air Quality e-Reporting database. Specifically, O_3 hourly values (µg/m^3) for all hours of the years 2022 and 2023 have been used.

Chemical transport modelling outputs

The CAMS Ensemble Forecast model outputs as provided by the Copernicus Atmosphere Monitoring Service (CAMS) at a regional scale over Europe have been used (CAMS, 2024), i.e. the ensemble of eleven involved air quality modelling outputs. Specifically, hourly O_3 values (µg/m^3) for all hours of the years 2022 and 2023 at a spatial resolution of 0.1° x 0.1° have been used. For details, see Horálek et al. (2024, 2025).

Meteorological parameters

The meteorological data used are the ECWMF data extracted from the CDS (Climate Data Store, https://cds.climate.copernicus.eu/cdsapp#!/home). Hourly data for 2022 and 2023 are used. Most of the data come from the reanalysed data set ERA5-Land at a 0.1°x0.1° resolution (of CDS), namely the indicators:

Surface solar radiation (MWs/m^2) – variable "Surface solar radiation downwards",
Temperature (K) – variable "2m temperature",
Surface pressure (Pa) – variable "surface_pressure",
Soil water – variable "Volumetric soil water layer 3", i.e. layer of 28-100 cm
Relative humidity – calculated based on variables "2m temperature" and "2m dewpoint temperature" (see below Eq. A1.7),
Wind speed (m/s) – calculated based on variables "10m u-component of wind" and "10m v-component of wind" (see below Eq. A1.8).

Relative humidity is derived by means of the saturated water vapour pressure (e_t) as a function of the indicators "2m temperature" (T) and "2m dew point temperature" (D) according to relation

$$RH = \frac{e_D}{e_T} = \frac{0.611 \cdot \exp\left(\frac{17.502 \cdot D}{240.97+D}\right)}{0.611 \cdot \exp\left(\frac{17.502 \cdot T}{240.97+T}\right)} = \frac{\exp\left(\frac{17.502 \cdot D}{240.97+D}\right)}{\exp\left(\frac{17.502 \cdot T}{240.97+T}\right)}, \qquad \text{(A1.7)}$$

where *RH* is the relative humidity,
D is the dew point temperature at 2 meter height,
T is the temperature at 2 meter height.

([4]) The United Kingdom exited the European Union in January 2020 and does not report air quality data to the AQ e-reporting database. Nevertheless, in order to enable the interpolation across the whole mapping domain, the publicly available British data from the Defra database have also been used in the analysis.

Wind speed (WV) is derived from the “10m u-component of wind” (10U) and “10m v-component of wind” (10V) according to relation

$$WV = \sqrt{(10U)^2 + (10V)^2} \qquad \text{(A1.8)}$$

In the coastal areas (where the data from ERA5-Land are not available), the same parameters from the reanalysed data set ERA5 in 0.25°x0.25° resolution are applied. Next to this, the following data (not available in the ERA5-Land data set) from the ERA5 data set is also used:

Friction velocity (m/s) – variable “Friction velocity”. The friction velocity (also known as the shear-stress velocity) has the dimensions of velocity.
Surface sensible heat flux (W/m^2) – variable “surface_sensible_heat_flux”.

Altitude

The altitude data field (in meters) of Global Multi-resolution Terrain Elevation Data 2010 (GMTED2010) is used, with an original grid resolution of 15 arcseconds see Danielson and Gesch (2011). The data were re-gridded converted into the reference EEA 1 km resolution grid, see Horálek et al. (2024).

Soil hydraulic properties data

JRC data called "Maps of indicators of soil hydraulic properties for Europe" in 1 km resolution are used for POD calculations, JRC (2016). Namely the following indicators are used:

Wilting Point – water content at wilting point (cm^3/cm^3),
Field Capacity – water content at field capacity (cm^3/cm^3).

A2.2 Land cover data

CORINE Land Cover 2018 (CLC2018) – 100 m resolution, Version 2020_20 is used (EU, 2020). For areas missing in this database (i.e. Andorra, Jan Mayen and some border areas), MDA (2015) and ESA (2019) land cover data resampled to 100m resolution have been used. For details, see Horálek et al. (2024).

A2.3 Agricultural data

For determining the area covered by wheat and potato, the agricultural data for 2022 in 2 km resolution as applied in Schucht et al. (2024) have been used, i.e. the EUROSTAT wheat and potato production data spatialized from the NUTS-2 level to the 2 km grid resolution using the CLC2018 data of level-3 classes 2.1.1 “Non-irrigated arable land”, 2.4.1 “Annual crops associated with permanent crops”, 2.4.2 “Complex cultivation patterns”, and 2.4.3 “Land principally occupied by agriculture, with significant areas of natural vegetation”. For details, see Schucht et al. (2024).

Annex 3 Results of the POD_Y analysis for biogeographical regions

This Annex 3 is related to Chapter 5. Similar results as presented in Chapter 5 at the country level (see Figures 5.2 to 5.8) are presented here at the level of the biogeographical regions.

Figure A3.1 (related to Figures 5.2 to 5.6 showing results for countries) presents the inter-annual differences between years 2022 and 2023 for POD_3_ref and the different contributions of the limitation functions. Figures A3.2 and A3.3 (related to Figures 5.7 to 5.8 presenting results for countries) show heatmaps of POD_3_ref and heatmaps of the different contributions of the limitation functions for years 2022 and 2023.

Figure A3.1 POD_3_ref Inter-annual variation 2023-2022 of POD_3_ref for wheat in mmol/m² (left) and efficiency of the limitation functions for its reduction in % (right), biogeographical regions, in mmol/m² PLA

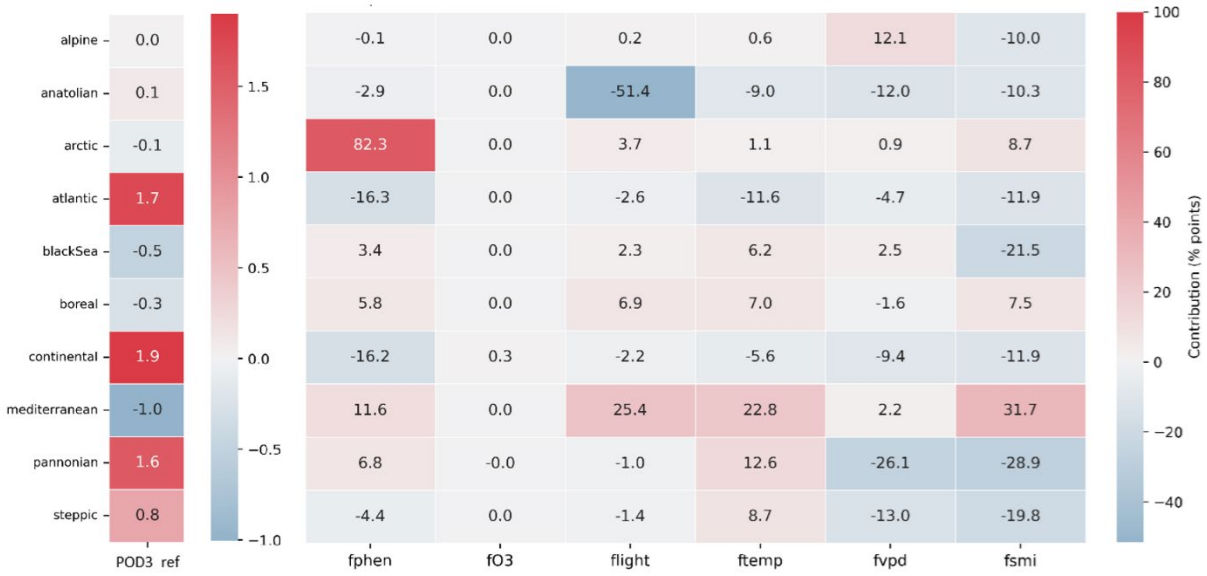

Figure A3.2 POD_3_ref for wheat in mmol/m² PLA (left) and efficiency of the limitation functions for its reduction in % (right) in 2022 for biogeographical regions

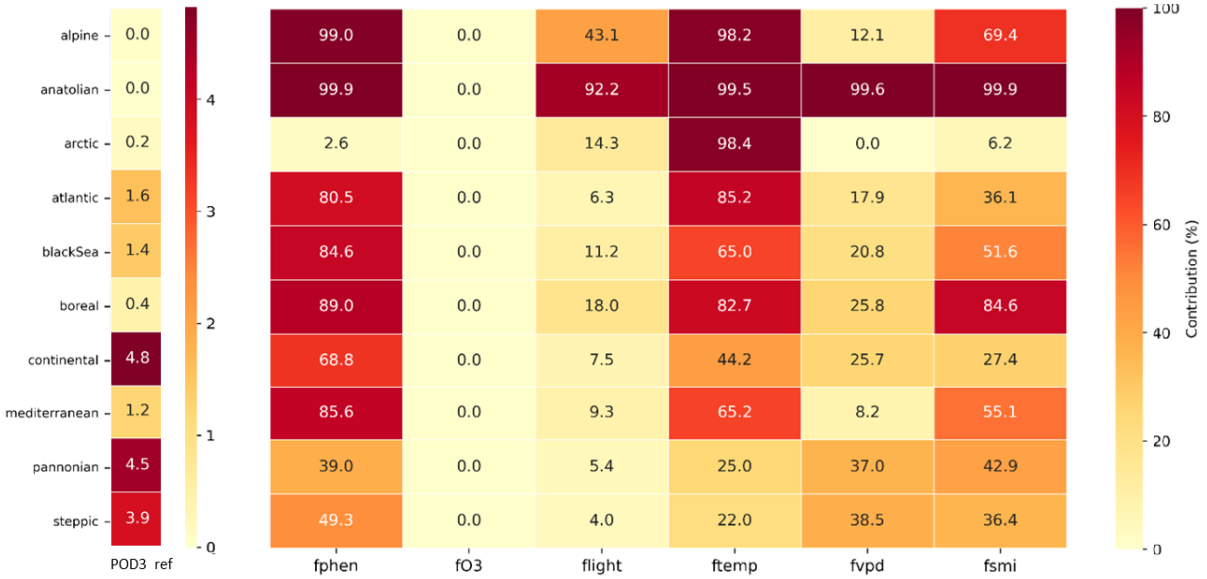

Figure A3.3 POD_3_ref for wheat in mmol/m² PLA (left) and efficiency of the limitation funcitons for its reduction in % (right) in 2023 for biogeographical regions

European Topic Centre on
Human health and the environment
https://www.eionet.europa.eu/etcs/etc-he

The European Topic Centre on Human health and the environment (ETC HE) is a consortium of European institutes under contract of the European Environment Agency.

European Environment Agency
European Topic Centre
Human health and the environment